AN ANALYSIS OF THE HYDROTHERMAL FLUID CHEMISTRY AND ISOTOPIC DATA OF YELLOWSTONE LAKE VENTS

Master's Thesis

SUBMITTED TO THE FACULTY OF THE

UNIVERSITY OF MINNESOTA

By

Christie D. Cino

IN PARTIAL FULFILLMENT OF THE REQUIREMENTS

FOR THE DEGREE OF

MASTER OF SCIENCE

Advisor: Dr. William E. Seyfried

May, 2018

ACKNOWLEDGEMENTS

First and foremost I would like to thank my advisor, William E. Seyfried Jr., for his guidance, encouragement, and support during the development of this work. His brilliance and curiosity motivated me to continuously learn and discover more about my research. Also, the skills I developed from the experience I gained in the Aqueous Geochemistry lab has been invaluable. I have never learned so much from a single person, and I appreciate all you have done for me these past few years.

I would like to thank Chunyang Tan for always going above and beyond to help me with any technical issue I had. Beyond your vital contributions to this project, road tripping with you to Yellowstone was a blast! I would also like to thank the members of the Aqueous Geochemistry lab for all their support – Peter Scheuermann, Andrew Fowler, and Elizabeth Lundstrom. Of course, I also am deeply thankful to the HD-YLAKE team for creating and funding this project. This research would not have been possible without you all!

I am grateful to my committee members, Cara Santelli, Brandy Toner, and David Kohlstedt. Thank you for always answering any questions I may have had during class or for my research, and all your efforts to help me succeed throughout my education!

To my family and friends – my deepest tanks for all your love and support throughout the years. Whenever I didn't believe in myself anymore, you all were always there to pick me back up. I am especially grateful to my dad Sal, even from a thousand mile distance I could always feel you rooting for me. You are my biggest fan! Lastly, to my cats Luna, Quincy, Lily, and Leia for keeping me company during the long nights of reading and writing.

ABSTRACT

Yellowstone National Park is a dynamic environment home to an array of geysers, hot springs, and hydrothermal vents fueled by the underlying continental magmatic intrusion. Yellowstone Lake vent fluids accounts for approximately 10% of the total geothermal flux for all of Yellowstone National Park. Though studying this remote hydrothermal system poses severe challenges, it provides an excellent natural laboratory to research hydrothermal fluids that undergo higher pressure and temperature conditions in an environment largely shielded from atmospheric oxygen. The location of these vents also provides chemistry that is characteristic of fluids deeper in the Yellowstone hydrothermal system. In August 2016 and 2017, hydrothermal fluids were collected from the Stevenson Island vents in collaboration with the Hydrothermal Dynamics of Yellowstone Lake (HD-YLAKE) project using novel sampling techniques and monitoring instrumentation. The newly built ROV Yogi was deployed to reach the vents in-situ with temperatures in excess of 151^{o}C at 100-120 m depth, equipped with a 12-cylinder isobaric sampler to collect the hydrothermal fluids.

Analyses of the Yellowstone Lake hydrothermal fluid revealed chemistry almost identical to that of the lake water, with the exception of an abundance of dissolved gases, such as CO_2 and H_2S. Dissolved H_2 and CO are also present, suggesting more reducing conditions at elevated temperatures with high fractions of hydrothermal source fluid. Reducing conditions are also indicated by high H_2S/SO_4 ratio, and in-situ chemical sensor data. A particularly abnormal feat of these fluids is the dissolved silica concentrations, which are well below saturation with respect to quartz and amorphous silica, in spite of the silica-rich substrate which the hydrothermal fluids vent through. One explanation for this chemical data is influx of high enthalpy steam from a boiling zone immediately beneath the lake floor. Mass-balance calculations indicate the collected sample contain 27% vapor to mix with lake water in order to achieve the observed temperatures of the vent fluids. However, this interpretation is a paradigm shift from the previous models, which entail mixing of a chloride rich, isotopically heavy deep thermal reservoir liquid with lake water.

TABLE OF CONTENTS

LIST OF TABLES

LIST OF FIGURES

CHAPTER 1

INTRODUCTION

1.1 Geologic and Geophysical Background

Yellowstone National Park is one of the most active hydrothermal and tectonic systems on Earth, with nearly half of the world's geysers and related geothermal phenomena. These systems are fueled by heat and mass transfer associated with magmatic intrusions intrinsic to the origin and evolution of the Yellowstone caldera. Unlike tectonic volcanism at divergent plate boundaries and subduction zones, the Yellowstone volcanic system results from an underlying intraplate hotspot. Intraplate hotspots have long been attributed to hot, buoyant plumes of magma rising from deep within the Earth, (Morgan, 1971; Crough, 1978, 1983; Burov et al., 2007). Multiple studies suggest that the Snake River Plain is an extension of Yellowstone Plateau, and resulted from the passage of the North American Plate over the hot spot (Figure 1) (Morgan, 1971, 1972; Matthews and Anderson, 1973; Smith and Sbar, 1974; Armstrong et al., 1975; Smith, 1977; Bonnichsen, 1982; Leeman, 1982; Morgan et al., 1984; Pierce and Morgan, 1990, 1992; Kuntz et al., 1992; Smith and Braile, 1994; Morgan et al. 1995; DeNosaquo et al., 2009; Rodgers et al., 1990). As the North American plate migrated to the southwest and volcanic activity shifted to northern regions, the extinct rhyolitic calderas gradually subsided to their current elevations (2.7 km at western boundary to 0.1 km at mouth) due to thermal and gravitational forces, thus shaping the Snake River Plain's path (Pierce & Morgan, 1992). The Yellowstone region evolved into its current state through three almost identical volcanic cycles. Each of these cycles began and ended with long periods of irregular lava eruptions, with a brief climax of catastrophic eruptions in between (Christiansen, 1984;

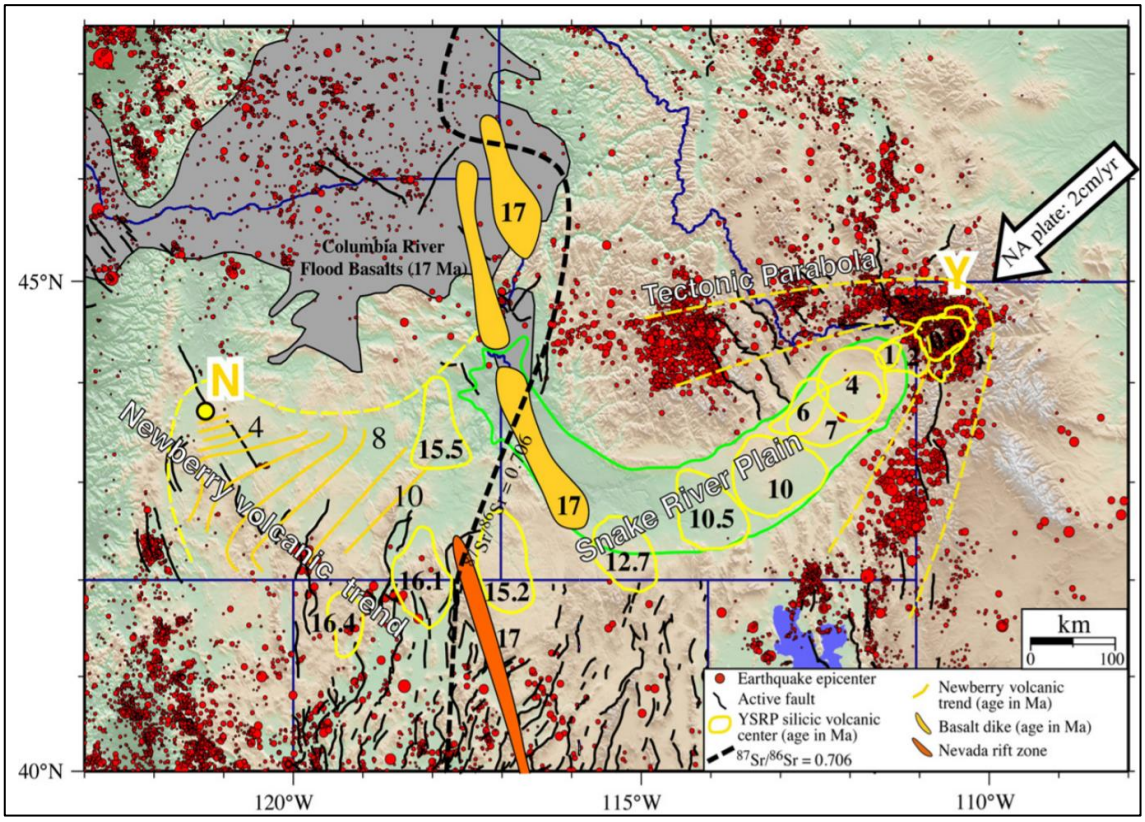

Figure 1 *– Track of the Yellowstone Hotspot in Mya from Smith et al. (2009). This figure shows the relative motion of age-transgressive ESRP silicic volcanic centers, opposite of the direction of the North American plate motion (white arrow).*

Christiansen et al., 2007). Ash flow spread hundreds of kilometers around the caldera after each climax event, and by the end of all three cycles, rhyolite covered hundreds of square kilometers, while the ash layers covered half of North America. This caused the underlying magma chamber to be partially emptied, resulting in their lithospheric roofs collapsing forming giant calderas (Christiansen, 1984). However, each subsequent volcanic event would partly fill the previously made caldera with lava, along with have a lot of overlapping surface, making them difficult to distinguish.

The Yellowstone magmatic evolution was extensively studied by Christiansen (1984), who proposed the existence of multiple eruptions that occur in cycles contributing to the formation of the Yellowstone Plateau. The first cycle eruption (2.1 myr.) is believed to be the largest of the three. This eruption formed a single cooling unit with a volume of

2500 km^3, now called the Huckleberry Ridge Tuff (Christiansen 1984). Due to the complete absence of any erosional features or sediment accumulations in this giant ash sheet, it must have cooled very quickly, estimated to be on the order of a few hours to days (Christiansen 1984). The caldera formed from this event extended Yellowstone Plateau to Island Park, but is now obscured by younger volcanic rocks and deposits. The second volcanic event was smaller in magnitude, but still catastrophic nonetheless. The eruption caused a single, fast-cooling unit just like the first cycle's, though much smaller in size (280 km^3), called the Mesa Falls Tuft days (Christiansen 1984). Volcanism from the second cycle was fully nested by the northern flank of the first cycle's caldera. The caldera formed from this eruption was 25 km across, and fully covered the area of the first cycle's caldera (Christiansen 1984). The third and final volcanic cycle began 1.2 million years ago, when volcanic activity shifted away from Island Park and became more localized to the Yellowstone Plateau we know today (Christiansen 1984). For about the first 600,000 years, intermittent rhyolitic lava eruptions occurred from arcuate fractures around the perimeter of the present Yellowstone caldera. These fractures were caused by a shallow crustal-level magma chamber that had a fluctuating doming and sagging roof structure from partial emptying of the chamber (Christiansen 1984). About 640,000 years ago the climatic eruption of the third cycle occurred and formed another single fast cooling ash unit with a volume of 1000 km^3, called the Lava Creek Tuff, which actually formed from two different ash flows that erupted simultaneously (Christiansen and Blank, 1972; Christiansen 1984). This was initially discovered through detailed stratigraphic studies, but further volcanic research found two shallow-crustal level magma chambers atop of a much larger underlying body of magma that erupted (Christiansen and Blank, 1972). The resulting

caldera encompassed the two intersecting ring-fracture zones formed by the collapsed chambers (Smith and Baily, 1968). However, shortly after their collapse the two chambers experience magmatic resurgence and formed two structural domes, the Sour Creek dome in the northeast part of the caldera, and the Mallard Lake dome in the south (Smith and Baily, 1968; Christiansen 1984).

The shallow low-velocity body (LVB) beneath the Yellowstone caldera has been imaged by the distortion of S and P waves as they propagated through the crust and upper mantle. This structure has been recognized to be purely an upper mantle phenomena in which buoyant and relatively viscous magma attached itself to the underside of the North America plate, called the residuum (Humphreys et al., 2000). The magma plume is sheared to the southwest against the southwest moving North America plate (Lowry et al., 2000), producing an elongate plume head beneath the Snake River Plain and Yellowstone Plateau. A silicic magma chamber extending from this residuum resides from 8-10 km below the Yellowstone caldera (Humphreys et al., 2000). A basaltic intrusion partially melted the surrounding rhyolitic rocks, which enriched the melt in silica (Hildreth, 1981). At a further depths of 20-50 km in the lower to middle crust, a larger basaltic magma reservoir was recently revealed by using a joint tomographic inversion of local and teleseismic earthquake data (Huang et al., 2015). The hydrothermal system at Yellowstone caps this magmatic system, which fuels the convective circulation of the subsurface water supply.

The overall permeability structure in which the hydrothermal fluid circulates in both sub-lacustrine and sub-areal regions includes primarily rhyolitic lava flows (Morgan and Shanks, 2005). Sedimentary rocks are also present originating from the Paleozoic and Mesozoic, however, there are areas of alternating permeable and impermeable volcanic

units, which may create deep thermal water reservoirs that cannot ascend effectively (Fournier, 1989; Shanks and Morgan 2005). Thus, fluid travels laterally beneath the impermeable units, to fracture zones that allow fluids to escape, creating abundant hydrothermal activity along the lava flow perimeter (Shanks and Morgan 2005). The majority of hydrothermal fluid in Yellowstone originates as meteoric water which isotopically resembles local rain water that recharged groundwater from centuries ago (Craig, 1956; Pearson and Truesdell, 1978; Kharaka et al., 2002; Rye and Truesdell, 2007). The cool "recharge" fluid slowly descends through the crust and passes into aquifers at the base of the volcanic pile. In the central caldera the fluid is then heated to approximately 360°C by contact with high temperature rhyolites, which causes the fluid to ascend to shallower aquifers, reacting with rocks in the wall column, while mixing with meteoric and pore water from the surface (Fournier, 1989). These thermal waters can undergo minor or extensive reactions with the surrounding rocks, depending on the residence time of the water in the convective system.

1.2 Previous Studies on Yellowstone Hydrothermal Fluids

1.2.1 Distribution of source fluids

A deep neutral-chloride thermal reservoir underlies all of the thermal systems in Yellowstone National Park, and is believed to undergo boiling from 360^{o}C to 220^{o}C (Truesdell et al., 1977; Fournier, 1989; Shanks et al., 2005). Phase separation, which is the conversion of a single-phase fluid into liquid and vapor components, occurs due to decompression of the putative source fluid at temperatures from approximately 180^{o}C to 270^{o}C. The liquid component typically contains abundant Cl^{-}, is often silica-rich with near neutral pH, and more often found at lower elevations within in the park (Allen and Day,

1935; White et al., 1971; Fournier, 1989; Hearn et al., 1990; Lowenstern et al., 2012). These waters are associated with sinter terraces, which are sloping plains of amorphous silica that typically have an abundance of biological mats of thermophile life that forms near hydrothermal pools (Brock, 1978; Braunstein and Lowe, 2001; Guidry and Chafetz, 2003).This neutral-chloride fluid is also characterized by high concentrations of alkali metals, boron, and arsenic. In contrast, the fumarolic steam is accompanied by significant amounts of volatile gases such as H_2S, CO_2, and NH_3, with negligible amounts of Cl^- (Fournier, 1989; Nordstrom et al., 2005; Inskeep et al., 2010; White et al., 1991; Allen and Day, 1935). Sub-aerial pools that receive this vapor become highly acidic due to the creation of sulfuric acid from the reaction of H_2S with atmospheric oxygen, and the addition of protons from the dissolution of CO_2 (Lowenstern et al., 2012; Xu et al., 1998). Evidence suggests that Yellowstone Lake has received both of these types of fluid, just at different times. For instance, the hydrothermal fluid that diffused from the Bridge Bay vents 11 ka ago from silicified conduits likely composed of the neutral, Cl^--rich water (Shanks et al., 2005). The silicified conduits could only form if the hydrothermal fluid is saturated in silica, enabling it to precipitate once it ascends and cools. . However, Stevenson Island vents and Mary Bay vents found in the deep hole are likely dominated by vapor, due to the lack of any silicified conduits near the vents (Balistrieri et al., 2007; Shanks et al., 2005).

1.2.2. Vapor-dominated systems in Yellowstone

Vapor-dominated systems are characterized by steam and other gases, such as CO_2 and H_2S, ascending a significant vertical extent though fractures beneath an impermeable cap that acts as a throttle (Fournier 1989, White et al., 1971). This type of system essentially

acts as a heat pipe, with the rising vapor transferring heat to the surface with minimal amounts of liquid water. Formation of liquid water condensate, however, is a necessary by-product of heat transfer within vapor-dominated systems, Steam condensate then flows back downward under the influence of gravity. Around the impermeable cap atop the vapor-dominated system, there is often a zone of perched water that is a mixture of local meteoric water and condensed steam (Fournier, 1989). The existence of a hydrostatically underpressured system like this requires either that the vapor-dominated region lies in a topographically high terrain to be perched above the surrounding lowlands in topographically high terrain or an area of relatively low permeability surrounds the vapor-dominated zone, which effectively prevents any free movement of cold groundwater into the system (White et al., 1971; Fournier, 1989; Schubert et al., 1980; Schubert and Strauss, 1980; Raharjo et al., 2016).

Typical surface features of vapor-dominated systems include fumaroles, mud pots, acid-sulfate boiling pools that contain little chloride with virtually no visible discharge of liquid water, and barren landscapes composed predominantly of residual quartz, clays, sulfates, and native sulfur (Fournier 1989; Raharjo et al., 2017). Additionally, there is a complete absence of nearby alkaline-chloride thermal waters. These features are commonly found throughout much of the relatively high plateau region in the east-central part of Yellowstone National Park, suggesting s a vapor-dominated system underling much of this region (White et al., 1997). A vapor-dominated system has been confirmed in the Mud Volcano region through drilling research (White et al., 1975, Zohdy et al., 1973), which is just 8 km north of Yellowstone Lake. Chemical geothermometry has been carried out by Fournier 1981 on these subaerial fluids, which indicates temperatures of about 180-190°C

for water-rock interactions within this vapor-dominated system. Additionally, relatively high concentrations of ammonia have also been found in these acid-sulfate waters in the eastern part of YNP, with the predominant dissolved constituent being ammonium sulfate (Fournier, 1989). H_2S also travels with the steam, which oxidizes once it reaches the surface and reacts with atmospheric oxygen, producing the abundant sulfate and low pH characteristic of these waters (White el al., 1971; Hurwitz et al., 2012).

1.2.3 Origins of geothermal gases

Isotopic studies suggest gases and other volatile elements represent a mixture of components derived from magmatic, crustal, and meteoric sources. Carbon dioxide is mantle-derived by magmatic degassing, with minor amounts contributing from the crust that have generally similar $\delta^{13}C$-values as mantle carbon (Lowenstern et al., 2015; Horita, 2001; Werner and Brantely, 2003). The dominant sulfur isotopic composition of $\delta^{34}S$ values near 0 per mil, also seen in sulfate alteration minerals across Yellowstone, is consistent with oxidation of H_2S supplied from magmatic degassing (Lowenstern et al., 2015; Marini et al., 2011). However, the sulfate dissolved in neutral chloride waters is observed to be isotopically heavier, with $\delta^{34}S$ values ranging from +10‰ to +20‰ (Truesdell et al., 1978). Analysis of $^{13}C/^{12}C$ ratios, however, reveal that the decomposition of high molecular weight hydrocarbons from crustal-fluid interactions is the principal source for CH_4 and other organic gases (Des Marias et al., 1981; Lorenson and Kvenvolden, 1993; Bergfeld et al. 2011, 2012; Lowenstern et al., 2015). CH_4 is depleted in ^{13}C relative to the larger hydrocarbons, and if magmatic CH_4 were the source it would need at least equal, if not higher, ratios of $^{13}C/^{12}C$ relative to the chain hydrocarbons (Des Marias et al., 1981). Noble t gases such as Ar, N_2, and Ne are derived mostly from meteoric

water, however, helium (He) is a mixture of crustal and mantle sources (Kennedy et al., 1985; Lowenstern et al. 2015)

1.2.4 Yellowstone Lake

Yellowstone Lake is the largest high-altitude subalpine lake in the United States, situated at 2,357 m above sea level and covering 341 km^2 of the Earth's surface (Morgan et al., 2007). Currently the lake has more than 141 rivers adding water and sediment into Yellowstone Lake, with the Yellowstone River being the dominant contributor. The northern half of the lake resides inside the Yellowstone volcanic caldera (0.64 myr. event), and hosts more than 250 hydrothermal vents (Balistrieri et al., 2007). The western part of Yellowstone Lake, called West Thumb, lies within the West Thumb caldera that was formed 178,000 years ago from the 128-ka tuff of Bluff Point eruption (Christiansen et al., 1984; Morgan, L.A., and McIntosh, W.C., 1998). Yellowstone Lake is a dynamic environment in which there are multiple hydrothermal and tectonic processes continuously shaping the lake floor, which include currently active fault systems and hydrothermal explosion events that create large depressions (>500m diameter) in Yellowstone Lake (Wold et al., 1977; Morgan et al., 2003) and throughout the Park (Morgan et al., 2009). Multiple events can trigger hydrothermal explosions in Yellowstone Lake, such as the melting of glacial ice, seismic activity, and erosion, which may also affect coexisting hydrothermal vent activity (Rose, 2004). These events form from excessive steam/CO_2 pressure build up and release, and are a significant geologic hazard in the park (Christiansen et al., 2007; Lowenstern et al., 2005; Morgan et al. 2007). Mary Bay, the

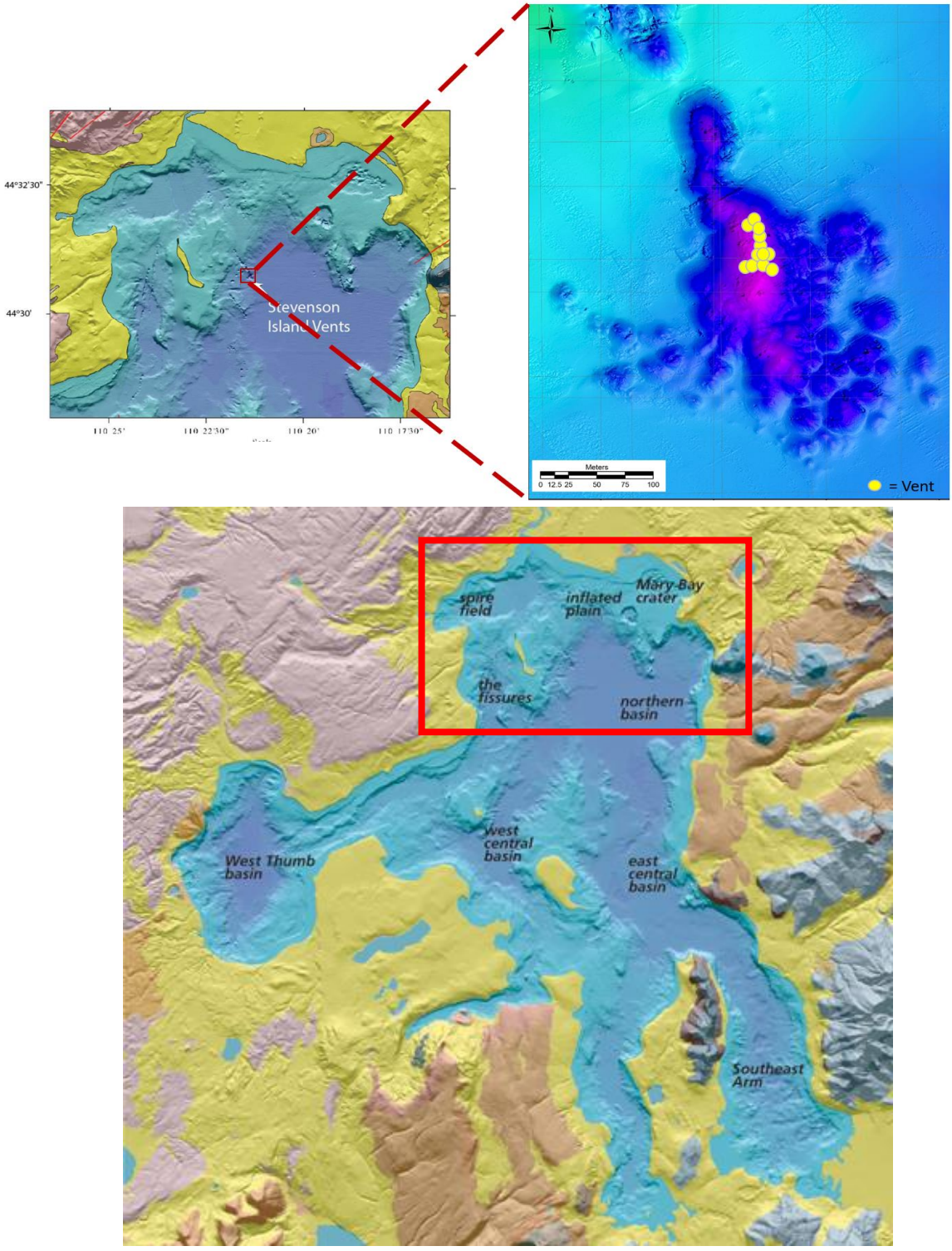

Figure 2 *– (left) Diagram of the north-eastern section of Yellowstone Lake modified from Shanks et al. 2007, and (right) a bathymetry map of the Stevenson Island vent field. Yellow circles represent vents that were sampled in August 2016 by the HD-YLAKE project (bottom). Map of major locations in Yellowstone Lake from USGS.*

largest know hydrothermal explosion crater in the world at 2.5 km diameter, excavated rock from a hydrothermal system that may have extended as deep as 540 m, estimated by isotopic evidence found in fluid inclusions from mineralized veins in Mary Bay breccia (Morgan et al., 2009). Currently, in the northern basin of Yellowstone Lake, there is much evidence, such as high heat flow, ongoing seismic activity, active deformation, explosion craters, that suggests abundant hydrothermal activity (Morgan et al., 2009).

Though the lake floor is difficult to access, it provides an excellent natural laboratory to research connections between magmatic, tectonic, climatic, and hydrothermal processes that are highly sensitive to perturbations. Our field site is in the north-eastern part of Yellowstone Lake, and east of Stevenson Island, called the "Stevenson Island vents" (Figure 2). The Stevenson Island vents are situated atop of northwest trending fissures east of Stevenson Island (Morgan et al., 2007), along with dozens of hydrothermal explosion craters. The hydrothermal vents are not associated with chimney-like structures on the lake floor, but rather fluids are diffusively issuing from conduits created by dissolution of clay-rich sediment. This description generally agrees with the observations of Shanks et al. (2007), which are based on previous sampling of hydrothermal vent fluid throughout Yellowstone Lake (Balistrieri et al., 2007).

1.3 Purpose of Study

Continental hydrothermal systems are a primary source of geothermal energy, economically important metal deposits, provide support for exotic ecosystems, while posing a significant geological hazard. Yellowstone National Park is one of the world's largest continental hydrothermal systems, and the Yellowstone Lake vent fields represent a significant component of YNP geothermal energy budget. The goal of the Hydrothermal

Dynamics of Yellowstone Lake (HD-YLAKE) project is to understand how earthquakes, volcanic processes, and climate affect the widely unexplored hydrothermal system located beneath Yellowstone Lake. There are many processes that affect the chemical evolution of hydrothermal fluid, such as phase separation, water–rock and water-sediment interactions, biological processes, and magmatic degassing. Our goal is to better characterize these reactions through geochemical analysis of hydrothermal fluid samples. Observing the cause-and-effect relationships between frequent perturbations and hydrothermal flow can facilitate a better understanding of the subsurface processes that are otherwise difficult to observe.

The research group at University of Minnesota has developed a novel gastight hydrothermal fluid sampling system, which can acquire fluid samples at elevated lake floor vent sites. The sampler is made of titanium and includes 12 gastight chambers with a manifold inlet system. An in-situ chemical sensor was also developed to monitor pH and redox conditions in real time at a number of vent sites, making it a key component in locating quality vent fluid samples for geochemical and biological analysis.

CHAPTER 2

METHODOLOGY

2.1 Sample collection and processing

2.1.1 Collection of hydrothermal fluid

To access the hydrothermal vents on the bottom of Yellowstone Lake, HD-YLAKE project had use of the newly designed and recently developed ROV Yogi (Figure 3) and support ship R/V Annie, which are owned and operated by the Global Foundation for Ocean Exploration. AUV exploration was conducted in advance of ROV deployment. The high-resolution bathymetry provided from this exploration facilitated the location of possible vent sites. The high temperature probe on the ROV was first used to explore the vent sites, then in-situ pH and redox measurements of vent fluids were made using solid state sensors designed to sustain the elevated temperatures and pressures. The small diameter of the high T probe, however, permitted deep penetration into the substrate of the vent system and always returned fluid temperatures higher than could be achieved by achieved by the thermocouple intrinsic to the larger pH and redox sensor wand (Figure 3). The sensor wand contained a YSZ membrane electrode with Ag/Ag_2O internal element

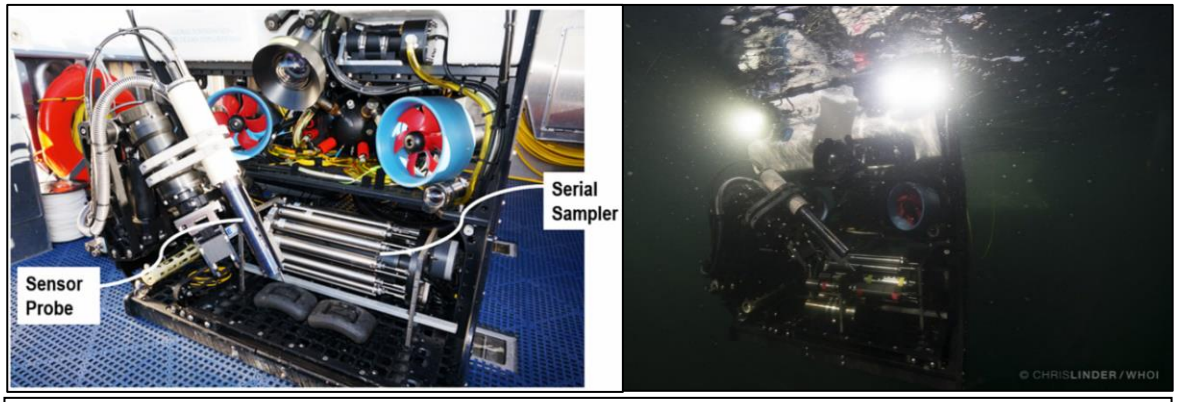

Figure 3 – *(left) Titanium, 12-cylinder serial sampler[2] and in-house designed YSZ membrane electrode on ROV Yogi in August 2016. ROV and R/V Annie owned and operated by Global Foundation for Ocean Exploration. (right) Picture of ROV Yogi submerged in Yellowstone Lake. Photo credit to Chris Linder.*

and internal pressure balanced Ag/AgCl reference electrode were used to measure pH, while a platinum electrode provided redox constraints (Tan et al., 2017). Positioning the sensor involved the use of the manipulator on the ROV, together with ICL (inductively coupled link) communication (Bradley et al., 2001; Ding and Seyfried, 2007). ICL enables non-contact communication between the sensor and ROV, allowing continuous, real time, chemical and temperature data transfer. This capability was key in finding high quality hydrothermal fluid samples, since the constant and instant data feedback was given as the sensor was positioned in hydrothermal fluid issuing from Yellowstone Lake vents. Hydrothermal fluid samples were then selectively collected with a titanium 12-cyclinder serial sampling device (Figure 3). Each chamber in the serial sampler had a back pressure of ~11 bars of nitrogen gas (a titanium piston separates the sample fluid reservoir from the back pressure media), which is slightly below the pressure at lake bottom at the vent site. However, in August 2017 field operations, pressurized de-ionized water was used as back pressure media to modulate the rate of fluid flow into the sampler, so as to preclude or minimize the amount of lake water entrained with the vent fluid. The sampler was attached

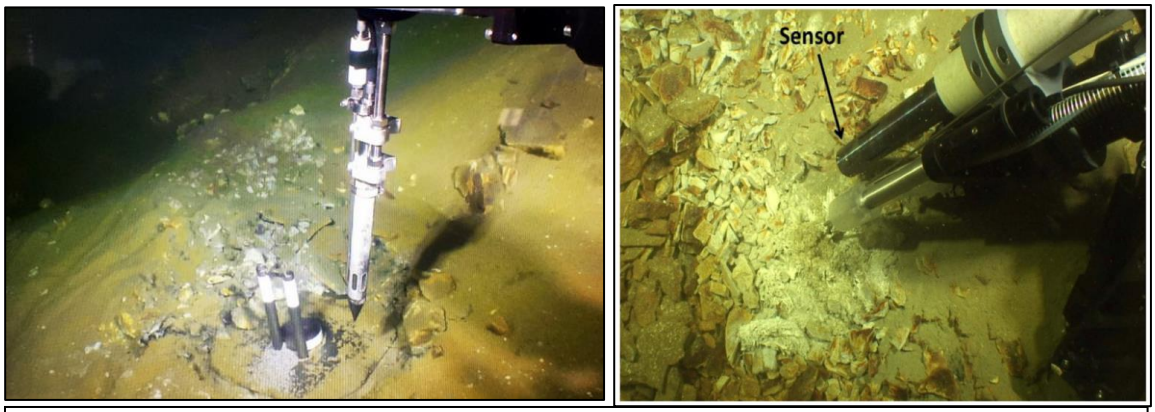

Figure 4 *– (left) snorkel used to collect vent fluid before being put into the insert during August 2017 field ops (right) Deployment of chemical sensor unit at a vent at 115m depth near the Stevenson Island study site during August 2016 field ops, from Tan et al. (2017). All vents that the hydrothermal fluid issued diffusively from semilithified conduits, likely formed by dissolution of subsurface rock and lake bed sediments, which largely consist of diatomaceous material (Shanks et al.,2007).*

to a snorkel (Figure 4), which was positioned as deeply as possible in the vent fluid discharge zone. In the field season of August 2017, an insert was put in the hydrothermal vents to streamline the fluid diffusively flowing out of the conduits to ease the sampling process (Figure 4).

2.1.2 Sample preparation and storage

Within hours of acquisition, all vent fluid from the pressurized titanium sampler was subsampled into syringes by activation of a high-pressure metering valve. Each sample cylinder had ~2mL extracted as rinse to avoid contamination effects, subsequently 5mL was taken to measure pH using a gel electrode and alkalinity values via an alkalinity titration (see Appendix) as a standard procedure. The pH was recorded immediately after stabilization, and though affected by CO_2 degassing, is likely close to the minimum value. Preliminary dissolved chloride concentration values of samples were measured using Chloride QuanTab® Test Strips, 30-600 mg/L to help identify a potential high quality liquid endmember sample, which is an extreme end component of a fluid mixture in terms of purity.

Aliquots for the major dissolved components (Na, Mg, Ca, K, Cl, SiO_2, SO_4, Br), minor species (Fe, Mn, Li, Sr, Rb), trace metals (B, Al, V, Cu, Zn, As, Rb, Zr, Mo, Ag, Cd, Sb, Cs, W, Pb) and dissolved silica were prepared by filtering 15-20 mL of hydrothermal fluid through 0.22 μm polyethersulfone (PES) syringe filters, and adding the fluid into pre-weighed, acid-washed low-density polyethylene (LDPE) bottles. In the metals aliquot, 50 uL ultra-pure Optima^{TM} HCl was added to acidify the solution to pH <2 to prevent any precipitation on storage. The silica aliquot was prepared by diluting the hydrothermal fluid from the metals aliquot by 25x in order to also prevent any potential

precipitation. The “majors” aliquot did not require any additional preparation as there was no threat of precipitation for the species of interest.

Dissolved gas samples were prepared by extracting ~5-10 mL of hydrothermal fluid from the sampler into an air-tight syringe, which was then injected into nitrogen-filled (N_2) amber bottles, that were slightly over-pressured from 1 atm. Attached to the injection syringes are 0.22μm polytetrafluoroethylene (PTFE) filters that were pre-soaked with acetone to allow the passage of gases before insertion of the hydrothermal fluid into the amber bottles. All amber bottles were acid-washed in 2N HCl, then flushed with N_2 to remove any oxygen. Blue chlorobutyl septum stoppers were used to seal the bottles that were sanitized in boiling 2N NaOH, and then secured with aluminum retainers. A vacuum was made in the field on the amber bottles that is proportional to the amount of hydrothermal fluid to be added.

Dissolved sulfide samples were prepared by injecting 40-50 mL of hydrothermal source fluid through 0.22 μm PES syringe filters into pre-evacuated amber bottles containing 0.5g of zinc acetate. ZnS was then extracted from the fluid samples through a second round of filtration later in the laboratory at University of Minnesota. Carbon isotope samples were prepared by extracting 50 mL of hydrothermal fluid from the sampler into a large, air-tight syringe and injecting it into a pre-evacuated amber bottles that contained 200 μL of saturated mercury chloride ($HgCl_2$) for microbial sterilization (Wolf et al., 1989). The amber bottle and septum stopper preparation is the same as described for dissolved gasses, except the bottles were previously evacuated using a vacuum pump.

The hydrogen and oxygen isotope samples were prepared by extracting ~5.5 mL of vent fluid from the sampler into a gas-tight syringe. The fluid was then injecting through a

0.22 μm PES filter into plastic air-tight vails. All air bubbles were removed from the samples during injection to prevent evaporation effects. To accomplish this, the sample vial was filled completely with vent fluid. Analysis for these isotopes then proceeded within the next few months due to long term storage over a year in plastic containers changes up to +5‰ for δD, and +2.0‰ for $\delta^{18}O$ (Spangenberg, 2012).

2.2 Geochemical analyses of hydrothermal fluid

2.2.1 In-situ temperature, pH, and redox conditions

In-situ measurements were accomplished by in-house developed solid state sensors, which contained a yittria stabilized zirconia (YSZ) membrane electrode for pH measurements (Tan et al., 2017; Neidrach et al., 1980; Zhang and Charles, 2003; Macdonald and Zhu, 2005) and a platinum electrode for redox conditions. First, the temperature probe equipped on the ROV was used for reconnaissance of the vent site. Deployment of the chemical sensors involved initial stabilization in the vent fluid flow by positioning the unit at the base of the fluid discharge zone. As the sensor measured temperature, it asymptotically approached a constant maximum temperature and eventually stabilized, which also caused the electrochemical potential recorded by pH and redox sensors to stabilize. Further details about the sensor design can be found in Tan et al., (2017).

2.2.2 Major chemistry

Elemental chemistry analyses incorporates major anions, cations, and heavy metals present in the hydrothermal fluids. Anions were analyzed using ion chromatography (IC), cations using inductively coupled plasma optical emission spectrometry (ICP-OES), and heavy metals using inductively coupled plasma mass spectrometry (ICP-MS). All analyses

were processed in the Analytical Geochemistry lab at the University of Minnesota. The analytical uncertainty from replicate analysis and instrumental error is ±3% for Na, Cl, Ca, K, SO_4, Mg, SiO_2 and Sr; ±5% for Li, Fe, Mn; and ±10% for Br.

2.2.3 Dissolved gases

Dissolved gas concentrations (CH_4 and CO_2) were analyzed using Agilent GC-with TCD/FID detection. Gas chromatography allows measurement of the concentration of these gases in the headspace of our samples. Henry's law is used to calculate the aqueous concentration of the gases, and the two fractions combined. Henry's Law is defined as:

$$C_{(aq)} = \frac{p_{(gas)}}{k_H} \quad (1)$$

Where $C_{(aq)}$ is the concentration of the of the solute in the solution, $p_{(gas)}$ is the partial pressure of the solute above the solution, and k_H is the Henry's law constant (Table 1), which differs depending on the solute.. Gas was extracted by an air-tight syringe from the slightly over-pressured sample bottles. The overpressure allowed the syringe to keep extracting air up until it equilibrium with the atmosphere (1 atm). Accuracy of plastic syringes used to extract gas from the bottle headspace is typically within ±2% of actual volume under 1 atm at 25ºC. Analytical uncertainty for dissolved gasses is ±5% for ΣCO_2, CH_4, CO, and H_2.

Table 1 – Henry's law constant for selected gases from Sander (1999).

Gas	K_H (M/atm)
CO_2	3.4×10^{-2}
CH_4	1.3×10^{-3}
H_2	7.8×10^{-4}
CO	8.7×10^{-4}

2.2.4 Sulfide Concentrations

Hydrogen sulfide (H_2S) concentrations were analyzed gravimetrically by trapping the sulfide into crystalline zinc sulfide (ZnS) precipitate from solid zinc acetate, and then performing a chemical conversion to silver sulfide (Ag_2S) (see Appendix). After the conversion was finished, the Ag_2S was filtered out of the trapping solution and dried in an

oven (100 °C) for gravimetric and future isotopic analyses. The analytical uncertainty for the sulfide samples is ±7%.

2.2.5 Carbon Isotopes

The compound-specific carbon isotope analysis of dissolved gases was conducted by a gas chromatography-combustion-isotope ratio mass spectrometer (GC-C-IRMS) system at University of Houston. The GC (Trace GC Ultra, Thermo Scientific) was configured with a 30 m capillary PoraPLOT Q column (Agilent). It was connected to a Delta V IRMS (Thermo Scientific) through a combustion furnace running at 940^{o}C. The temperature step-heating program for GC started at 45^{o}C (hold for 2 min), and ramped to 210^{o}C with 50^{o}C per minute (hold for 12 min). UHP helium (99.999%) was used as a carrier gas at a split flow rate of 12 mL/min with split ratio of 3:1. This analytical process is a well-documented technique that separates organic compounds using on-line continuous flow with GC followed by combustion and analysis of ^{13}C with IRMS (Hayes et al., 1990; Merrit et al., 1994). Carbon and sulfur stable isotope data for each isotope of interest, A, are reported in standard delta notation (δA) expressed as:

$$\delta A\ (‰) = \left[\frac{R_S - R_{STD}}{R_{STD}} \right] \times 1000 \qquad (2)$$

where R_S and R_{STD} are the isotope ratios (^{13}C/^{12}C) of the sample and the standard, respectively. Analytical uncertainty is ±0.2‰ for all samples.

2.2.6 Water Isotopes

Deuterium/Hydrogen (D/H) and Oxygen-18/Oxygen-16 (^{18}O/^{16}O) were analyzed at the U.S. Geological Survey in Denver, Colorado, using a Picarro system (Model 2130i, cavity ring-down spectrometer). This device uses a tunable laser to separate and quantify isotopic abundance in the water molecule (Gupta, 2009). Analyses were calibrated using

accepted international (IAEA, Coplen et al., 2002) standards (VSMOW, SLAP, GISP) and several working standards of local waters. Samples were analyzed multiple times and run in groups with similar isotope values to minimize memory affects during analysis. Uncertainties were calculated by replicate analyses of samples and standards gives standard deviations (1σ) of better than ±0.3‰ for δD and ±0.05‰ for $\delta^{18}O$.

CHAPTER 3

RESULTS

3.1 In-situ temperature and pH

Hydrothermal fluids from Yellowstone Lake vents were collected during two field seasons, the first in August 2016, and the second in August 2017. The highest temperature recorded was 174^{o}C by the Alvin high temperature probe, the hottest fluid to ever be measured in Yellowstone National Park. In August 2016, a peak vent fluid temperature of 160^{o}C during fluid sampling was measured, with an average range of 120-150^{o}C (See Table A.1). One low temperature fluid of 63^{o}C was taken, along with three samples of bottom lake water (BLW). In August 2017 almost all the fluid collection occurred between 140^{o}C-150^{o}C. In-situ pH readings for the 2016 sample collection ranged from 4.2-4.5 (Tan et al., 2017), and remained within this range for 2017.

3.2 Chemical data

Table 2a – Chemical data for selected cations in Yellowstone Lake vent fluid

Vent Sample	Fe (µm/kg)	Mg (µm/kg)	K (µm/kg)	Na (µm/kg)	Ca (µm/kg)
YL16F01	2.1	101	45	391	122
YL16F02	1.7	95	43	369	111
YL16F03	0.9	98	45	394	115
YL16F05	16.5	105	41	350	135
YL16F06	12.2	180	53	357	170
YL16F07	35.3	110	39	381	141
YL16F08	0.9	88	42	367	109
YL16F09	6.1	182	47	372	172
YL16F10	3.3	134	44	360	142
YL16F11	13.5	96	41	354	120
YL16F12	1.1	87	39	342	107
YL16F13	0.4	93	43	372	118
YL16F14	1.1	100	44	381	119
YL17F01	1.4	88	39	346	124
YL17F02	4.0	89	38	342	121
YL17F03	3.8	123	41	344	131
YL17F08	1.6	111	43	385	144
BLW (AVG)	4.0	103	41	383	129

Table 2b – Chemical data for selected anions and dissolved silica in Yellowstone Lake vent fluid samples

Vent Sample	Cl (µm/kg)	F (µm/kg)	SiO_2 (µm/kg)	SO_4 (µm/kg)
YL16F01	139	33	165	121
YL16F02	122	33	187	237
YL16F03	133	34	188	166
YL16F05	106	21	157	95
YL16F06	114	22	251	115
YL16F07	124	25	107	82
YL16F08	111	35	237	116
YL16F09	124	18	202	102
YL16F10	114	25	181	101
YL16F11	114	26	124	94
YL16F12	109	32	203	105
YL16F13	113	32	171	100
YL16F14	119	31	241	130
YL17F01	102	25	194	146
YL17F02	103	24	191	159
YL17F03	110	17	200	172
YL17F08	128	24	125	128
BLW (AVG)	122	28	98	92

Table 3 – Chemical and isotopic data for selected volatiles in Yellowstone Lake vent fluid

Vent Sample	H_2S (mm/kg)	CO_2 (mm/kg)	CH_4 (μm/kg)	C^{13}-CO_2 (‰)	C^{13}-CH_4 (‰)
YL16F01	0.32	0.8	19	N/A	N/A
YL16F02	0.45	3.6	31	N/A	N/A
YL16F03	0.18	2.8	30	N/A	N/A
YL16F05	N/A	2.1	41	N/A	N/A
YL16F06	N/A	5.3	77	N/A	N/A
YL16F07	1.87	14.1	161	-4.77	-53.27
YL16F08	0.50	7.5	96	N/A	N/A
YL16F09	0.20	8.6	109	N/A	N/A
YL16F10	1.20	6.7	47	-7.32	-64.05
YL16F11	N/A	12.0	220	N/A	N/A
YL16F12	2.10	6.3	66	-6.19	-65.41
YL16F13	0.43	2.9	22	N/A	N/A
YL16F14	N/A	6.0	39	N/A	N/A
YL17F01	1.02	17.2	141	N/A	N/A
YL17F02	1.05	12.2	114	N/A	N/A
YL17F03	1.28	10.8	163	N/A	N/A
YL17F08	0.68	13.0	193	N/A	N/A
YL17F010	N/A	12.2	118	N/A	N/A

*****H_2 and CO were detected in sample YL17F01 with concentrations of 31.0 μm/kg and 2.5 μm/kg, respectively

Measured Cl^- contents ranged from 102 µm/kg to 139 µm/kg, which is roughly the same as the bottom Yellowstone lake water, which averages approximately 122 µm/kg. The same is true for all dissolved cations. (Figure 5). Fe contents ranged from 0.39 µm/kg to 35 µm/kg, but this range includes the lake water average value of 4 µm/kg (Fig. 8). Dissolved F^- is the only element in the vent fluid samples that is depleted in comparison to the lake water. In contrast, all dissolved volatile species are elevated in concentration compared to the lake water. Total dissolved CO_2 ($\sum CO_2$) reached a value of 17 mm/kg, while dissolved H_2S ranged from 0.18 mm/kg to 2.1 mm/kg, with lower temperature samples having the lower H_2S concentrations. These H_2S concentrations drastically surpassed the dissolved SO_4^{2-} values in the vent fluids, which range from 82 µm/kg to 237 µm/kg. This range is elevated compared with Yellowstone Lake water (Table 2b), likely due to H_2S oxidation effects. Dissolved CH_4 is enriched in vent fluid samples, with values

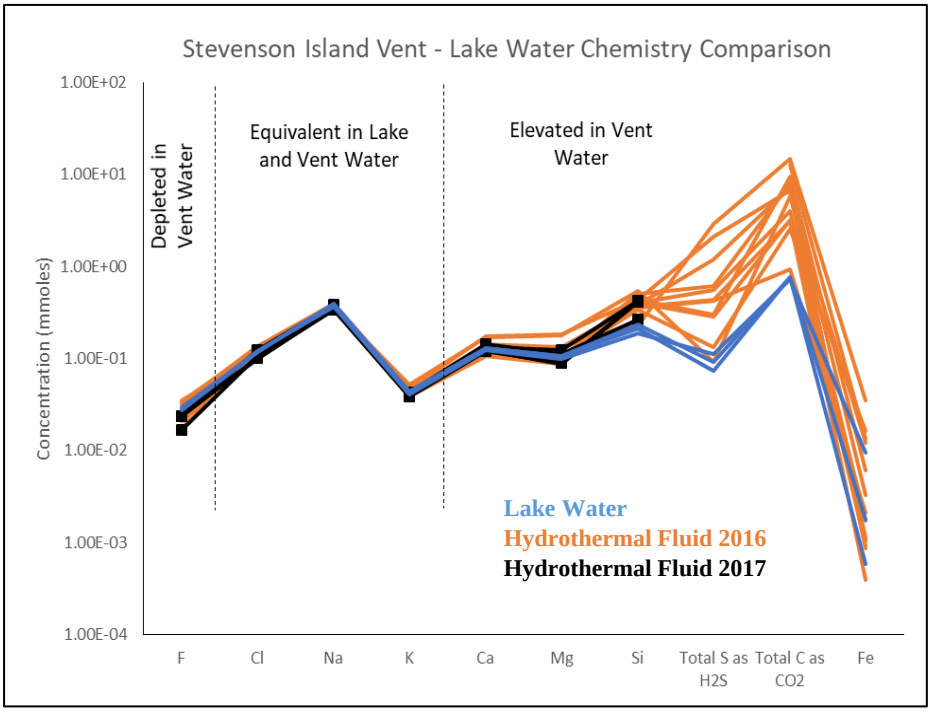

Figure 5 *– Geochemical composition of collected hydrothermal fluid in comparison to the bottom lake water. The hydrothermal fluid is enriched in gaseous components, such as CO_2 and H_2S, whereas ionic chemistry is similar to lake water.*

that range from 19 μm/kg in the lowest temperature fluid samples to 219 μm/kg in a higher temperature fluid samples. CO and H_2 were detected in one fluid sample taken in 2017, with concentrations of 2.5 μm/kg and 31.0 μm/kg respectively. This same sample has the highest value of $\sum CO_2$, (17.2 mm/kg), which suggests correspondence between temperatures, total dissolved CO_2 and reducing conditions.

3.3 Carbon, hydrogen and oxygen stable isotopes

The $\delta^{13}C$ isotopic data for $\sum CO_2$ varied from -4.77‰ to -7.32‰. The sample in the lower range (-4.77‰) corresponds with higher temperature, and therefore is the more accurate representative for the isotopic signature of the endmember fluid. CH_4 $\delta^{13}C$ ranged

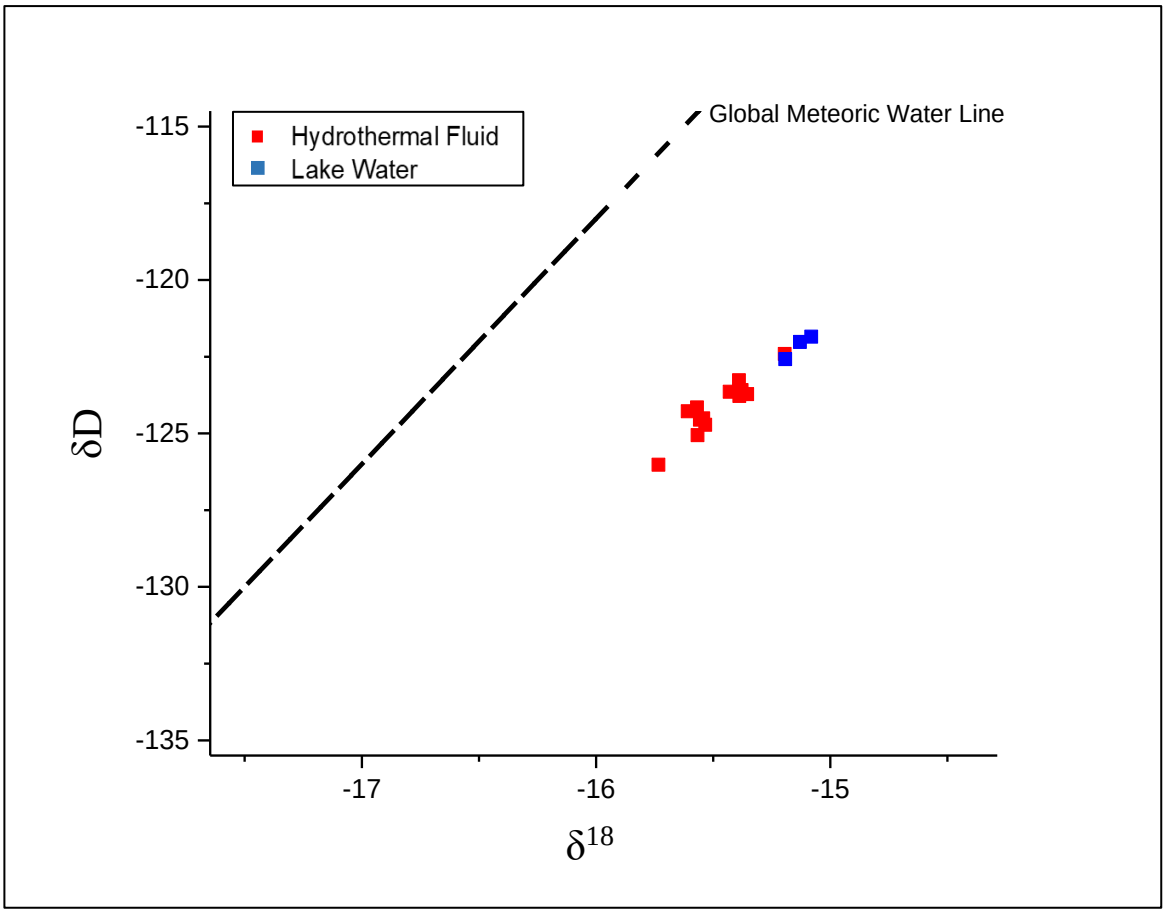

Figure 6 *– Deuterium and oxygen isotopes composition for Stevenson Island hydrothermal fluids and bottom lake water. Other relevant fluids plotted from data by Balistrieri et al. (2004)*

from -53.26‰ to -65.41‰, again with the heavier values being more representative of the endmember fluid.

δD and $\delta^{18}O$ values varied from -121.85‰ to -126.02‰, and -15.08‰ to -15.57‰ respectively (Figure 6). The lesser variability of $\delta^{18}O$ results from mass balance constraints in mineral-fluid systems (Taylor, 1978). The average bottom lake water δD and $\delta^{18}O$ values are -122.15‰ and -15.13‰, respectively. These values deviate from the hydrothermal fluid values, with the hydrothermal fluids being significantly lighter for both δD and $\delta^{18}O$. This is consistent with isotopic fractionation during boiling. δD and $\delta^{18}O$ isotope analyses also indicate that Yellowstone Lake waters and hydrothermal vent fluids plot off the global meteoric water line of Craig (1961) (Figure 6).

3.4 Endmember fluid calculations

The high enthalpy, low Cl, low SiO_2, and light deuterium values of the vent fluids strongly suggests the existence of a vapor-dominated system. Owing to uncertainties in the composition of the hydrothermal source fluid for Yellowstone Lake vents, a reasonable approach to estimate the relative abundance of hydrothermal fluid and Lake-water in composite vent fluid samples, involves the use of calculations based on enthalpy. It is well known that in any mixing process between hot and cold fluid, enthalpy is entirely conservative (ref). Thus, the fraction of hot hydrothermal and cold lake water can be estimated as follows:

$$H_T = xH_L + (1-x)H_V \quad (3)$$

Where H_T is the enthalpy of the hydrothermal fluid, H_L is the enthalpy of the lake water, H_v is the enthalpy of the ascending hot source fluid component (vapor), while x is the fraction of lake water. Enthalpy values were obtained using steam tables (Wagner and

Kretzschmar, 2008), and calculations were performed under the assumption of saturated stream at Yellowstone Lake bottom conditions of 12 bars pressure and 188°C. H_T and H_L values are known since the temperatures of these fluids were measured directly. However, the value of H_v needed to be estimated based on the pressure and temperature conditions allowed beneath Yellowstone Lake, since these parameters for the vapor have not yet been measured. The fraction of lake water (x) is estimated to be 0.73, making the proportion of vapor (1-x) to be 0.27.

CHAPTER 4

DISCUSSION

Overall, the composition of Stevenson Island vent fluids are remarkable similar to lake water, which as emphasized above, is consistent with heat transport by steam and the formation of a vapor dominated hydrothermal systems. The conspicuous abundance of dissolved volcanic gases, such as CO_2 and H_2S is largely in keeping with this assessment. Total dissolved CO_2 ($\sum CO_2$) concentrations increase linearly with temperature, suggesting a value of ~19 mmol/kg at a temperature of 174ºC, the highest temperature observed for the Yellowstone Lake vent system (see above) (Figure 7). Samples taken from the vents in 2017 generally have a higher proportion of hydrothermal fluid, with only two samples from 2016 falling within a similar range. In comparison, the solubility of CO_2 at 174ºC and 12 bars (pressure at the Yellowstone Lake floor) is approximately 28 mm/kg (Duan and Sun, 2003). A number of factors may account for the apparent difference between the calculated and measured dissolved CO_2 concentrations (Tan et al. 2017). Importantly, the temperature recorded by the thermocouple at the tip of the vent fluid sampler snorkel typically reported temperatures lower than the maximum

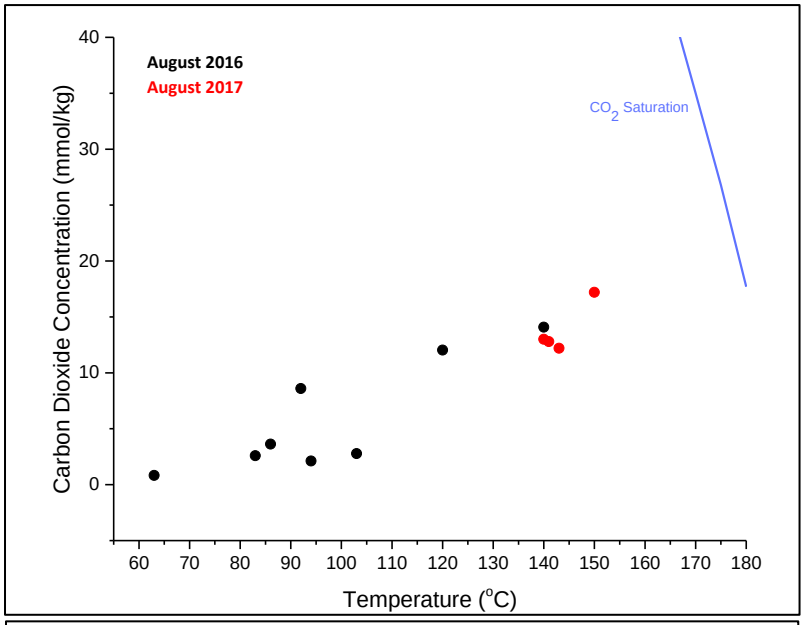

Figure 7 *– Measured total dissolved CO_2 concentrations for the Stephenson Island hydrothermal vents, in comparison to CO_2 saturation calculated from Duan and Sun (2003).*

observed temperature by the ROV temperature probe. This implies that our sampler snorkel also sampled the hydrothermal fluids lower than the maximum temperatures measured due to the physical inability to reach the deeper, hotter fluids from size limitations. We speculate that CO_2 loss from the fluid samples were caused by lake water and/or condensate mixing, since the fumarolic steam is not pure CO_2 (Lowenstern et al., 2012) which likely results in lower CO_2 solubility than calculated by Duan and Sun (2003). The occurrence of CO_2 degassing prior to sampling could also contribute to CO_2 loss. The lake bottom vent environment reveals abundant CO_2-rich gas bubbles that diffuse around the vents, which supports our interpretation of CO_2-degassing of saturated fluids prior to sampling. Previous CO_2 flux studies indicate that most Yellowstone vents are CO_2 saturated in the shallow subsurface over a wide depth–temperature range (Lowenstern and Hurwitz, 2008). Based on $\delta^{13}C$-CO_2 and CO_2/He data, the dominant source of CO_2 for the Yellowstone magmatic-hydrothermal system originates from the mantle, with lesser amounts potentially derived from sedimentary deposits (Lowenstern et al., 2015; Werner and Brantley, 2003). Hydrolysis of CO_2 is the likely source of the moderately low pH of the hydrothermal fluids issuing from vents on the lake floor.

The CH_4 concentrations agree with previously measured values from other hydrothermal vents in Yellowstone Lake by Innskeep et al. (2015). However, Innskeep et al. (2015) measured molecular hydrogen (H_2) concentrations of approximately 0.050-2.2 μm/kg, whereas most of our samples were below these values, the highest temperature vent fluid sample from the 2017 study was considerably higher, with a value of 31 μm/kg. This same sample also revealed dissolved CO (2.5 μm/kg) and had the highest concentration of CO_2 (17.2 mm/kg). Clearly, dissolved gas concentrations are extremely sensitive to

temperature change, and in the case of H_2 and CO, likely re-equilibrate rapidly at lower temperature, effectively removing these species from the vent fluid prior to sampling.

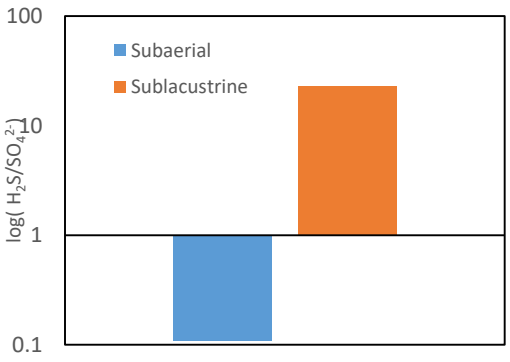

Figure 8 *– H_2S/SO_4^{2-} concentration ratios for average subaerial (Xu et al., 2000) geysers and the sublacustrine Yellowstone Lake vent fluids*

H_2S concentrations have not been previously measured for the hydrothermal fluids in Yellowstone Lake. However, studies of subaerial hydrothermal fluids indicate dissolved H_2S concentrations far below the 1-2 mm/kg concentrations reported here (Table xx). Accordingly, the high H_2S/SO_4^{2-} ratio for Yellowstone Lake vent fluids suggest moderately reducing conditions (Figure 8), which clearly differs from the redox environment in the subaerial vents (Xu et al., 2000). Due to the lack of atmospheric oxygen, the H_2S remains reduced and does not significantly contribute the hydrothermal fluid's acidity. These findings are consistent with the relatively low redox potential of 0.2 to -0.3V measured by chemical sensor (Tan et al., 2017). However, the measured vent fluid H_2S/SO_4^{2-} ratio deviates from that predicted from the chemical sensor data. This is likely due to the presence of other redox pairs, causing mixed potentials. Numerous studies have convincingly demonstrated a lack of internal equilibrium between redox couples in groundwater and hydrothermal fluids, which also depart from an overall measured redox potential (Grenthe et al., 1992; Stefansson et al., 2005; Stefansson and Arnorsson, 2002; Stumm and Morgan, 1996). Though we cannot currently provide unambiguous evidence that links the presence of multiple redox pairs to our measured redox potential, our data has made clear these hydrothermal fluids carry distinctly reducing redox conditions which

certainly helps drive the metabolism of the diverse microbiota living on the Yellowstone Lake bottom.

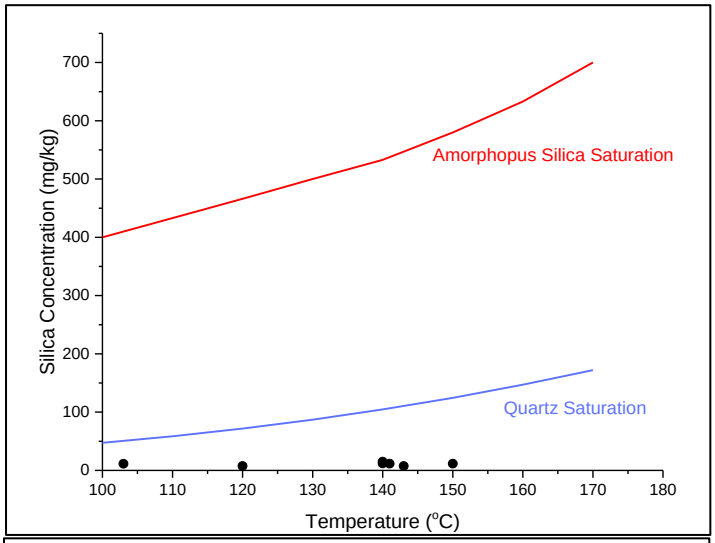

Figure 9 *– Yellowstone Lake hydrothermal fluid silica concentration in comparison with quartz and amorphous silica saturation at 12 bars*

Dissolved SiO_2 concentrations are elevated in the hydrothermal fluid, ranging from 107 µm/kg – 251 µm/kg. In comparison, the average bottom lake water concentration is 98 µm/kg. However, the concentrations in the vent fluid are highly under-saturated relative to quartz and amorphous silica (Figure 9) This is an unusually low dissolved silica concentration in these hydrothermal fluids, especially for fluid percolating through diatomaceous sediment at elevated temperature and pressure (Shanks et al. 2005).. Also, spire formation would occur if these fluids were high in silica concentration, similar to what is found at the Bridge Bay sublacustrine vent sites which once had hot, upwelling SiO_2-saturated hydrothermal fluids precipite out SiO_2 once mixed with cold lake water, forming pure SiO_2 conduits (Shanks et al., 2007). Spires are completely absent from the Stevenson Island vent field, likely indicating heat transport by steam rather than liquid, making SiO_2 transport minimal due to the low solubility of silica in steam. Experimental studies by Rimstidt and Barnes (1980) demonstrate that at temperatures below 230°C, the rate constant (k) for quartz precipitation decreases drastically. At temperatures below 100°C, the precipitation rates drop rapidly to extremely low values. Thus, the low SiO_2

content in the vent fluid and lack of silicified conduits is not unexpected. Even after the steam and pore water mix in the lake subsurface, there is probably insufficient opportunity to dissolve diatoms and ever achieve quartz saturation, let alone amorphous silica saturation.

The composition of Yellowstone Lake vent fluids are broadly consistent with the geochemistry of vapor dominated hydrothermal systems, as emphasized above. In the subareal environment, this is most often reflected by formation of so-called "acid-sulfate waters", which represents a mixture of condensed fumarolic steam and perched dilute groundwater (Nordstrom et al., 2009). The upflowing steam systems has abundant CO_2 with minor H_2S (Fournier 1989; Lowenstern and Hurwitz, 2008; Lowenstern et al., 2015). The contributions of SO_4 that characterizes acid-sulfate waters in Yellowstone Lake is provided by its reduced form H_2S. The lake water shields the vent fluid from atmospheric oxygen, preventing the oxidation reaction to occur. The low chloride and overall elemental content in these hydrothermal fluids attributes to their poor solubility in steam. There has been extensive experimental work that demonstrate most rock-forming minerals and elements are minimally soluble in steam below 250^{o}C, which includes MgO (Alexander et al. 1963; Maeda et al. 1978; Hashimoto 1992), CaO (Matsumoto & Sata 1981; Hashimoto 1992), Al_2O_3 (Hashimoto 1992), Co, Fe, Ni (Belton & Richardson 1962; Belton & Jordan 1967), and Morey 1957 for major metal oxides, SiO_2, and ZnS.

Previous models have interpreted the Yellowstone Lake hydrothermal system as a mixture of cold ambient lake water, and deep thermal reservoir fluid, which boils with steam loss from about 360°C to 220°C during ascent (Balistreri et al., 2007). This model was primarily d derived from the apparent linear relationship between dissolved Cl and δD

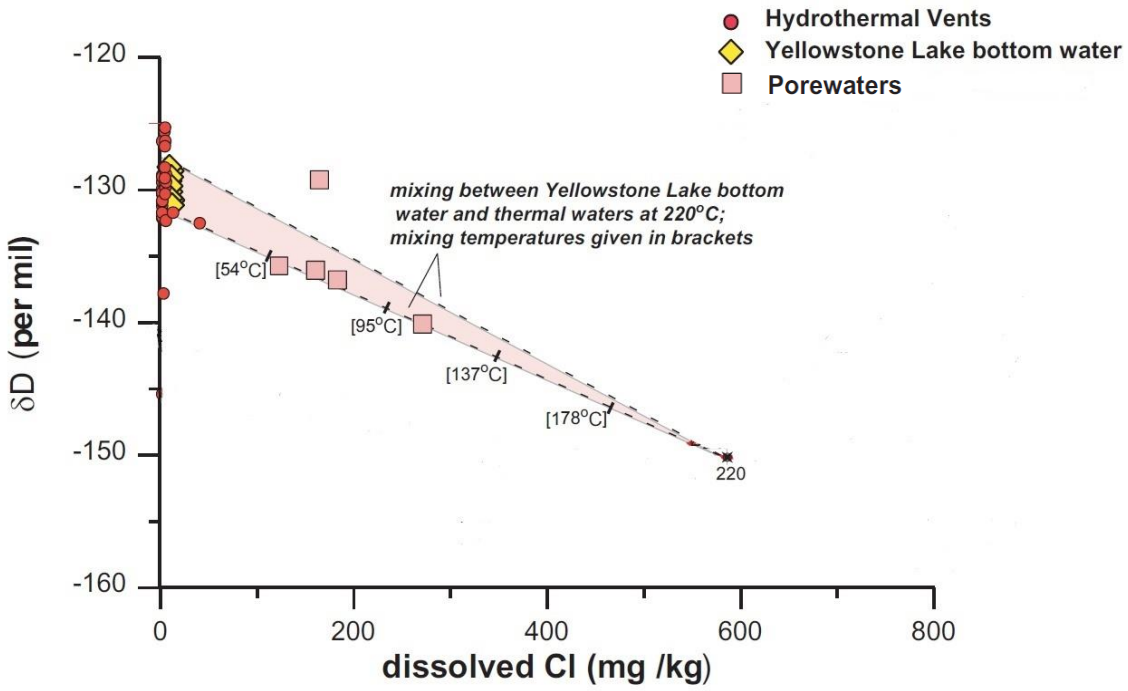

Figure 10 *- Plot of δD versus dissolved Cl concentrations derived from theoretical calculations and for data from inflow water, lake water, hydrothermal vent fluids, or pore waters in Yellowstone Lake. Diagram adapeted from Shanks et al. (2007), which was adapted from Truesdell and others (1977).*

(Figure 10), modified from the pioneering efforts of Truesdell et al., (1977). In this model, it is assumed that the dissolved Cl concentration of the hydrothermal source fluid is 16 mm/kg with a corresponding δD value of -150‰ (see Truesdell et al., 1977). This approach suggests that Yellowstone Lake is a mixture of 99% inflowing surface water, and only about 1% hydrothermal fluid (Balistreri et al., 2007). The model, however, is based largely on the chemical (Cl) and hydrogen isotope composition of pore fluids in West Thumb basin, which is in the western reaches of Yellowstone Lake. West Thumb basin formed separately from the rest of Yellowstone Lake during eruption of the ~140-ka tuff of Bluff Point (Obradovich, 1992), and subsequent collapse of the West Thumb caldera (Christiansen, 2001). These data can be interpreted to indicate that the West Thumb hydrothermal system may be disconnected from the rest of the hydrothermal system

beneath Yellowstone Lake and that caution should be applied when extrapolating the West Thumb data more broadly. An alternative interpretation involves mixing of high enthalpy and isotopically light and Cl depleted vapor with lake water isolated within a low permeability cap at/near the lake floor. Phase separation (vapor formation) must take place at temperatures less than 220ºC, consistent with constraints imposed by temperature dependent hydrogen and oxygen isotope fractionation data reported by Horita nd Wesolowski (1994).

The existence of low permeability cap rock is an essential feature of vapor-dominated hydrothermal systems (Schubert et al., 1980). In effect, this type of barrier assures that the escaping steam exceeds the pressure imposed by incoming liquids, while stabilizing the water over steam hydrologic system (Schubert et al., 1980; Schubert and Strauss, 1980; Raharjo et al., 2016). Since heat transport by steam is more efficient than it is for liquid water, only a fraction by mass of water is needed to achieve temperatures observed for Yellowstone Lake vent fluids at Stephenson Island. Enthalpy based mass balance calculations performed previously indicate vapor (steam) addition to lake water in a proportion of approximately 0.27:0.73. The enthalpy of the saturated steam is near its maximum of 2,500 kJ/kg for pure vapor (12 bar), while being relatively insensitive e to temperature and pressure changes (Fig. A.2).

Ingebritsen and Sorey (1988) proposed three conceptual models that illustrate the range of hydrothermal systems in which extensive vapor-dominated conditions are found. One model involves a reservoir surrounded by an impermeable shell, which may be representative of the vapor-dominated system in Yellowstone Lake due to the rock layers present beneath the surface. Two evolutionary pathways for this model were tested by their

simulations, which has be originally suggested by White et al. (1971). One pathway involves a decrease in mass inflow over time, and the other has conductive heating at a constant rate with no changes in boundary conditions. Though this configuration will be stable in a medium with a uniform low permeability, it can also be stable if pressures at the top of the vapor-dominated zone are slightly above local hydrostatic pressure (Schubert and Straus, 1980; Ingebritsen and Sorey, 1988).

Raharjo et al. (2017) mapped the permeability configurations that produce both liquid-dominated and vapor-dominated systems in permeability space. The simulation results produced five fields for geothermal systems, which included warm hydrostatic liquid-dominated, hot hydrostatic liquid dominated, over pressured liquid-dominated, early stage vapor zones, and lastly vapor-dominated systems. For vapor-dominated reservoirs to form, when the heat source is 8 MW/km^2, the cap rock permeability is restricted to range from 10^{-17} to $4 \times 10^{-16}\ m^2$, along with host-rock permeability having to be $5 \times 10^{-17}\ m^2$ or less (Raharjo et al., 2017). These results are consistent with previous modeling studies from Ingebritsen and Sorey, 1988, and the theoretical constraints given by Schubert et al., 1980. This narrow range is consistent with the rarity of vapor-dominated systems, since if the cap rock and the host rock are too impermeable, an overpressured liquid-dominated system is developed instead, and if they are overly permeable, a typical liquid hydrothermal system is formed.

As previously mentioned, the northern two-thirds of Yellowstone Lake is largely within the boundary of the 0.64 myr. Yellowstone Caldera (Eaton et al. 1975; Fournier 1989, 1999; Fournier et al. 1976; Lehman et al. 1982; Stanley et al. 1991; Wicks et al. 1998; Christiansen 2001). Morgan and Shanks (2005) created a convective flow model

emphasizing the role of post-caldera rhyolitic lava flows in Yellowstone Lake, and how these affect the distribution of hydrothermal features. This model suggests basal flow moves laterally through a more permeable unit below a 170-m-thick low-permeability un-fractured rhyolite flow to the fractured-flow margin, where the majority of hydrothermal activity is observed. This impermeable cap may allow steam to ascend to the lake bottom near the fracture zones, while obstructing lake water from entering the subsurface, and thus facilitating formation of a vapor-dominated hydrothermal system.

A notable feature found in the vapor-dominated reservoirs is the formation of such systems on pre-existing liquid-dominated hydrothermal systems, as indicated by patterns of alteration mineral formation (White 1971; Raharjo et al., 2017). There is evidence in parts of Yellowstone Lake, such as the spires in Bride Bay, which allude to past hydrothermal venting of a hot water system. These 12-15 spires are at a water depth of about 15 m, and extend to a height of 8 m with a diameter of 10 m (Shanks et al., 2005). Though currently inactive, isotopic studies using uranium-isotope disequilibria dated the spires to about 11 ka, shortly after the last glacial recession about 16 ka (Shanks et al., 2005). Though smaller siliceous conduits in the form of 1-8 cm diameter irregular tubes with 1-5 cm diameter openings have been found in Mary Bay, West Thumb, and east of Stevenson Island, these conduits likely formed within the sediment from diatom-fluid interactions Shanks et al., 2005). The hydrothermal fluid chemistry from these other vent sites look shockingly similar to the Stevenson Island vents, excluding the vent field from West Thumb (Balistrieri et al., 2007; Shanks et al., 2007). Thus, the hydrothermal system beneath Yellowstone Lake may currently be entirely vapor dominated, which likely evolved from a previous hot water system present thousands of years ago. Further

mineralogical studies of the Yellowstone Lake subsurface may provide useful insight on the evolution of the Yellowstone Lake hydrothermal system.

CHAPTER 5

CONCLUSIONS

The hydrothermal fluids issuing from vents at the bottom of Yellowstone Lake achieve the highest temperatures yet reported for venting fluids in Yellowstone National Park, measuring over 170°C. These high temperature vent fluids result in part from the high ambient pressure imposed by the water depth (~120 meters) in fault-related depressions in a region east of Stevenson Island. Novel technology involving ROV assets and newly designed high pressure vent fluid sampler, constructed entirely of titanium, as well as solid state chemical sensors, were successfully deployed. Analysis of the vent fluids surprisingly revealed chemical and isotopic properties not greatly different from the composition of deep Yellowstone Lake water, the high measured temperatures notwithstanding. Differences, however, do exist. In particular, dissolved chloride is noticeable less than lake water, while dissolved gases (CO_2, H_2S), are conspicuously higher. CO_2 is magmatically derived as indicated by carbon isotope data and a similar inference can be made for H_2S. In general, dissolved gas concentrations increase with increasing temperature. This is particularly noteworthy for CO_2, which strongly suggests saturation in the highest temperature vent fluid samples. Dissolved H_2 and CO is also present, suggesting more reducing conditions at elevated temperatures with high fractions of hydrothermal source fluid. Reducing conditions are also indicated by high H_2S/SO_4 ratio, and in-situ chemical sensor data. In spite of the silica rich substrate through which the hydrothermal fluids vent, dissolved silica concentrations are at trace levels, well below saturation with respect to quartz and especially amorphous silica.

The physical and chemical data from deep sublacustrine hydrothermal vents on the floor of Yellowstone Lake are best accounted for influx of high enthalpy steam from a boiling zone immediately beneath the lake floor. Calculations indicate that no more than ~25% steam is needed to mix with lake water to achieve the observed temperatures of the vent fluids. A result in general agreement with other chemical and isotopic data. This interpretation represents a paradigm shift from the previous models, which entail mixing of hot, chloride bearing, and isotopically heavy liquid with lake water. Volcanic-hosted vapor-dominated hydrothermal systems are rare due to the several requirements needed to produce a stable structure, which includes a robust heat supply and low permeability cap rock for the entire reservoir, which is several orders of magnitude lower than the permeability within the reservoir. The presence of extinct silica spires elsewhere in the Yellowstone Lake hydrothermal systems, provides evidence that liquid dominated systems have existed in past and perhaps presently as well, but require very different chemical and physical controls than presently in place for the deep vents near Stephenson Island.

The hydrothermal system of Yellowstone Plateaus is an unparalleled, dynamic environment that still has much to be discovered. Many of the different components making up Yellowstone National Park are interconnected to one another, and therefore affect the chemical, biological, and geological processes occurring at the park as a whole. Therefore, it is important to study their relationships in order to understand the integrated hydrothermal system associated with one of the most active volcanic provinces on Earth. Additionally, Yellowstone Lake is as an excellent natural laboratory to study sub-lacustrine hydrothermal systems previously present on other planetary bodies, such as Mars. The data available for any planetary environment is very limited compared to its terrestrial

counterparts, which makes studying Yellowstone as an analog is an excellent tool to better understand the extinct Martian hydrothermal system.

REFERENCES

Alexander C. A., Ogden J. S. and Levy A. (1963) Transpiration Study of Magnesium Oxide *J. Ch. Ph.* 39 (3057).

Allen, E.T., and Day, A.L. (1935) Hot springs of the Yellowstone National Park: Carnegie Institution of Washington Publication No. 466, 525

Armstrong, R.L., Leeman, W.P., Malde, H.E. (1975) K-Ar dating, Quaternary and Neogene volcanic rocks of the Snake River Plain Idaho. *Am. J. Sci*. 275, 225–251.

Balistrieri L. S., et al. (2007). The influence of sub-lacustrine hydrothermal vents on the geochemistry of Yellowstone Lake in Integrated Geoscience Studies in the Greater Yellowstone Area – Volcanic, Tectonic, and Hydrothermal Processes in the Yellowstone Geoecosystem. *U.S. Geological Survey Professional Paper.* 1717, 173–199

Belton G. R. and Richardson F. D. (1962) A volatile iron oxide. *Trans. Faraday Soc.* 58, 1562-1572

Belton G. R. and Jordan A. S. (1967) Gaseous hydroxides of cobalt and nickel. *J. Ph. Ch*. 71 (12), 4114–4120.

Bonnichsen, B. (1982) Rhyolite Lava Flows in the Bruneau-Jarbidge Eruptive Center, Southwestern Idaho. In: Bonnichsen, B., Breckenridge, R.M. (Eds.), *Cenozoic Geology of Idaho: Idaho Bureau of Mines and Geology Bulletin*, 26,283–320. Moscow, ID.

Braunstein, D., and D. R. Lowe (2001), Relationship between spring and geyser activity and the deposition and morphology of high temperature (>73°C) siliceous sinter, Yellowstone National Park, Wyoming, U.S.A. *J. Sediment Res.*, 71, 747–763.
Brock, T. D. (1978), *Thermophilic Microorganisms and Life at High Temperatures*, 465 pg., Springer-Verlag, New York.

Burov, E., Guillou-Frottier, L., d'Acremont, E., Le Pourhiet, L., Cloetingh, S., 2007. The plume head lithosphere interactions near intra-continental plate boundaries. Tectonophysics 434, 15–38.

Chiodini et al. (2012) Insights from fumarole gas geochemistry on the origin of hydrothermal fluids on the Yellowstone Plateau. *Geochem. Cosmchem.* 89, 265-278.

Christiansen, R. L. (1984) Yellowstone magmatic evolution: its bearing on understanding large-volume explosive volcanism. In Studies in Geophysics: Explosive Volcanism: Inception, Evolution, and Hazards, pp. 84-95. Washington, DC: Natl. Acad. Press

Coplon, J. K. et al. (2002) Isotope-abundence variations of selected elements. *Pure Appl. Chem.* 74 (10), 1987-2017

Craig, H. (1961) Isotopic variations in meteroic waters. *Science.* 133:1702–3.

Craig et al. (1963) Isotopic exchange effects in the evaporation of water: 1. Low-temperature experimental results. *J. Geophys. Reas.* 68 (17), 5079-5087.

Crough, S.T. (1978) Thermal origin of mid-plate hot-spot swells. Geophys. *J. R. Astron. Soc*. 55, 451–469.

DeNosaquo, K., Smith, R.B., Lowry, A.R. (2009) Density and lithospheric strength models of the Yellowstone-Snake River Plain volcanic system from gravity and heat flow data. *J. Volcanol. Geotherm. Res.* 188, 108–127.

DesMarais, D.J., et al. (1981) Molecular carbon evidence for the origin of geothermal hydrocarbons. Nature 292, 826–828.

Dickinson, W.R. (2004) Evolution of the North America Cordillera. *Annu. Rev. Earth. Planet. Sci.* 32, 13–45.

Duan, Z., and R. Sun. (2003) An improved model calculating CO_2 solubility in pure water and aqueous NaCl solutions from 273 to 533 K and from 0 to 2000 bar. *Chemical Geology.* 193, 57-271

Fournier, R. O. (1981) Application of water geochemistry to geothermal exploration and reservoir engineering. *In Geothermal Systems: Principles and Case Histories*, ed. L. Rybach, L. J. P. Muffler, New York: Wiley. 109, 43. New York: Wiley

Fournier, R.O. (1989) Geochemistry and Dyn-mics of the Yellowstone National Park Hydrothermal System. *Ann. Rev. Earth Planet. Sci.* 17, 13-53.

Fournier, R.O. (2007) Hydrothermal systems and volcano geochemistry. In: Dzurisin, D. (Ed.), Volcano deformation: Geodetic monitoring techniques. Springer, Berlin, 323–341 (Chapter 10).

Grenthe, I., Stumm, W., Laaksuharju, M., Nilsson A.C., and Wikberg P. (1992) Redox potential and redox reaction in deep groudwater systems. *Chem. Geol.* 98: 131-150.

Guidry, S. A., and H. S. Chafetz (2003) Depositional facies and diagenetic alteration in a relict siliceous hot-spring accumulation: Examples from Yellowstone National Park, U.S.A., *J. Sediment. Res.*, 71, 747–763.

Gupta, P., Noone, D., Galewsky, J., Sweeney, C., and Vaughn, B.H. (2009) Demonstration of high-precision continuous measurements of water vapor isotopologues in laboratory and remote field deployments using wavelength-scanned cavity ring-down spectroscopy (WS-CRDS) technology. *Rapid Commun. Mass Spectrom.* 23, 2534-2542.

Hashimoto A (1992) The effect of H2O gas on volatilities of planet-forming major elements: I. Experimental determination of thermodynamic properties of Ca-, Al-, and Si-hydroxide gas molecules and its application to the solar nebula. *Geochim. et Cosmochim*. 56 (1), 511-532

Hayes J. M., Freeman K. H., Popp B. N. and Hoham C. H. (1990) Compound-specific isotopic analyses: A novel tool for reconstruction of ancient biogeochemical processes. Org. Geochem. 16, 1115-1128.

Hildreth, W. (1981) Gradients in silicic magma chambers: Implications for lithospheric magmatism: *J. Geophys. Res*. 86, 10153–10192.

Horita, J. (2001) Carbon isotope exchange in the system CO_2-CH_4 at elevated temperatures. *Geochim. Cosmochim. Acta*. 65, 1907–1919.

Horita, J. and Wesolowski, D.J. (1994) Liquid-vapor fractionation of oxygen and hydrogen isotopes of water from the freezing to the critical temperature. *Geochim. Et Cosmochim.* 58 (16), 3425-3437.

Huang et al. (2015) The Yellowstone magmatic system from the mantle plume to the

upper crust. *Science.* 448 (6236), 773-776.
Humphreys, E. D., et al. (2000) Beneath Yellowstone: Evaluating plume and non-plume models using teleseismic images of the upper mantle. *GSA Today.* 10(12), 1–7.
Hurwtiz, S., et al. (2012) Temporal variations of geyser water chemistry in the Upper Geyser Basin, Yellowstone National Park, USA. *Geochem. Geophys. Geosyst.* 13(12), 1-19
Ingebritsen and Sorey (1988) Vapor-Dominated Zones Within Hydrothermal Systems: Evolution and Natural State. *J. Geophys. Rea.* 93 (B11), 13,635-13,655.
Inskeep et al. (2015) Geomicrobiology of sublacustrine thermal vents in Yellowstone Lake: geochemical controls on microbial community structure and function. *Front. Micro.* 6 (1044)
Jones, C.H., Unruh, J.R., Sonder, L.J. (1996) The role of gravitational potential energy in active deformation in the southwestern United States. Nature 381, 37–41
Kennedy, B.M., Lynch, M.A., Reynolds, J.H., and Smith, S.P. (1985) Intensive sampling of noble gases in fluids at Yellowstone, I. Early overview of the data, regional patterns. *Geochim. Cosmochim. Acta*. 49, 1251–1261.
Kuntz, M.A., Covington, H.R., Schorr, L.J. (1992) An overview of basaltic volcanism of the eastern Snake River Plain. In: Link, P.K., Kuntz, M.A., Platt, L.B. (Eds.), Regional Geology of Eastern Idaho and Western Wyoming. : Geo. Soc. Amer., Memoir, vol. 179. Geological Society of America, Boulder, CO, pp. 227–267.
Leeman, W.P. (1982) Development of the Snake River Plain-Yellowstone Plateau province, Idaho and Wyoming: An overview and petrologic model. In: Bonnichsen, B., Breckenridge, R.M. (Eds.), Cenozoic Geology of Idaho: Idaho Bureau of Mines and Geology Bulletin, vol. 26. Idaho Bureau of Mines and Geology, Moscow, ID, 155–178.
Lowenstern, J.B., and Hurwitz, S. (2008) Monitoring a Supervolcano in Repose: Heat and Volatile Flux at the Yellowstone Caldera. *Elements.* 4 (1), 35-40.
Lowenstern, J.B., et al. (2012) Generation and evolution of hydrothermal fluids at Yellowstone: Insights from the Heart Lake Geyser Basin. *Geochemistry, Geophysics, Geosystems.* 13(1), 1-20.
Lowenstern, J.B. et al. (2015) Origins of geothermal gases at Yellowstone. *J. Volcan. Geotherm. Rea.* 302, 87-101.
Lowry, A.R., Ribe, N.M., Smith, R.B. (2000) Dynamic elevation of the Cordillera, western United States. *J. Geophys. Res*. 105 (B10), 23,371–23,390.
Macdonald, D. D. and Zhu T. (2007) Current state-of-the-art in reference electrode technology for use in high subcritical and supercritical aqueous systems. in: R.W. Bosch (Eds.),Electrochemistry in Light Water Reactors Reference Electrodes, Measurement, Corrosion and Tribocorrosion, CRC Press, New York, p. 3–42.
Maeda E., Sasomoto T. and Sata T. (1978) Evaporation of magnesia in oxygen-water vapor atmosphere. *Yogyo-Kyokai-Shi*. 86, 491-499
Marini, L., Moretti, R., and Accornero, M. (2011) Sulfur isotopes in Magmatic-hydrothermal systems, melts and magmas. *Rev. Mineral. Geochem.* 73, 423–492.
Matsumoto K. and Sata T. (1981) A Study of the Calcium Oxide–Water Vapor System

by Means of the Transpiration Method. *Bull. Chem. Soc. Japan.* 54 (3), 674-677
Matthews, V., Anderson, C.E., 1973. Yellowstone convection plume and the break-up of the western United States. *Nature* 243, 158–159.
Merritt D. A., Brand W. A. and Hayes J. M. (1994) Isotope-ratio-monitoring gas chromatography-mass spectrometry: methods for isotopic calibration. *Org. Geochem.* 21, 573-583.
Morey G. W. (1957) The solubility of solids in gases. *Econ. Geol*. 52 (3), 225-251.
Morgan W.J. (1971) Convection plumes in the lower mantle. *Nature*. 230, 42–43.
Morgan, W.J. (1972) Plate motions and deep mantle convection. *Geol. Soc. Am. Memoir* 132, 7–22.
Morgan, L.A., Doherty, D.J., Leeman, W.P. (1984) Ignimbrites of the eastern Snake River Plain: Evidence for major caldera-forming eruptions. *J. Geophys. Res*. 89 (B10), 8665–8678.
Morgan, J.P., Morgan, W.J., Price, E. (1995) Hotspot melting generates both hotspot volcanism and a hotspot swell? *J. Geophys. Res.* 100, 8045–8062.
Morgan, L.A., et al. (2007) The floor of Yellowstone Lake is anything but quiet – new discoveries from high resolution sonar imaging, seismic-reflection profiling, and submersible studies. In: Morgan, L.A. (ed.), Integrated Geoscience Studies in the Greater Yellowstone Area – Volcanic, Tectonic, and Hydrothermal. Processes in the Yellowstone Geoecosystem. *US Geological Survey Professional Paper*. 1717, p. 95–126.
Morgan, L.A. and Shanks W.C. (2005) Influences of rhyolitic lava flows on hydrothermal processes in Yellowstone Lake and on the Yellowstone Plateau. Geothermal Biology and Geochemistry in Yellowstone national Park. 32-52.
Morgan, L.A., Shanks III, W.C., Pierce, K.L. (2009) Hydrothermal processes above the Yellowstone magma chamber: large hydrothermal systems and large hydrothermal explosions. The Geological Society of America Special Papers. 459, 1–95.
Niedrach, L.W (1980) A New Membrane-Type pH Sensor for Use in High Temperature-High Pressure Water. *J. Electrochem. Soc*. 127, p. 2122-2130.
Nordstrom, D.K., et al. (2005) Chemistry of thermal outflows in Yellowstone National Park. In *Geothermal Biology and Geochemistry in Yellowstone National Park*, edited by W.P. Inskeep and T.R. McDermott. 73-94
Nordstrom, D.K., McCleskey, R.B., Ball, J.W. (2009) Sulfur geochemistry of hydrothermal waters in Yellowstone National Park: IV Acid-sulfate waters. Appl. Geochem. 24, 191–207
Obradovich, J.D. (1992) Geochronology of the late Cenozoic volcanism of Yellowstone National Park and adjoining areas, Wyoming and Idaho: Open-File Report 92-408, 45 p.
Oduro, H. et al. (2011) Multiple sulfur isotope analysis of volatile organic sulfur compounds and their sulfonium precursors in coastal marine environments. *Marine Chemistry*. 124, p. 78–89
Pierce, K.L., Morgan, L.A. (1990) The track of the Yellowstone hotspot: Volcanism,

faulting, and uplift. *U.S. Geol. Surv. Open-File Report* 90-415. Geol. Surv, Denver, CO. 49 pp.
Pierce, K. L. and Morgan, L. A. (1992) The track of the Yellowstone hot spot: Volcanism, faulting, and uplift. *Regional Geology of Eastern Idaho and Western Wyoming: Geological Society of America Memoir*. 179, 1-53.
Rodgers, D.W., Hackett, W.R., and Ore, H.T. (1990) Extension of the Yellowstone Plateau, eastern Snake River Plain, and Owyhee plateau. *Geology.* 18(11), 1138-1141.
Raharjo, I.B., Allis, R.G., and Chapman, D.S. (2016) Volcano-hosted vapor-dominated geothermal systems in permeability space. *Geothermics.* 62, 22-32.
Rimstidt, J.D., and Barnes, H.L. (1980) The kinetics of silica-water reactions. *Geochim. et Cosmochim.*. 44, 1683-1699.
Rose, W.I. (2004) Natural hazards in El Salvador. *Geological Society of America.* 246–247
Sander, R. (1999) Compilation of Henry's Law constants for inorganic and organic species of potential importance in environmental chemistry. Germany, Rolf Sander. Schubert, G., Straus, J.M., and Grant, M.A. (1980) A problem posed by vapour-dominated geothermal systems. *Nature.* 287, 423-425.
Shanks et al, (2005) Hydrothermal vent fluids, siliceous hydrothermal deposits, and hydrothermally altered sediments in Yellowstone Lake. In *Geothermal Biology and Geochemistry in Yellowstone National Park,* edited by W.P. Inskeep and T.R. McDermott. 54-72.
Shanks III, W.C. et al. (2007) Geochemistry of sub lacustrine hydrothermal deposits in Yellowstone Lake: Hydrothermal reactions, stable isotope systematics, sinter deposition, and spire growth, in: Morgan, L.A. (Eds.), Integrated geoscience studies in the greater Yellowstone area: Volcanic, tectonic, and hydrothermal processes in the Yellowstone geoecosystem. U. S. G. S. Professional Paper, pp. 201-234.
Smith, R.B., 1977. Intraplate tectonics of the Western North American Plate. *Tectonophysics* 37, 323–336.
Smith, R.B., Sbar, M., (19740 Contemporary tectonics and seismicity of the Western United States with emphasis on the Intermountain Seismic Belt. *Geol. Soc. Am. Bull*. 85, 1205–1218.
Smith, R.B., Braile, L.W. (1994) The Yellowstone hotspot. J. Volcanol. Geotherm. Res. 61, 121–187
Sonder, L.J., Jones, C.H. (1999) Western United States Extension: How the West was widened. *Annu. Rev. Earth Planet. Sci.* 27, 417–462.
Spangenberg, J.E. (2012) Caution on the storage of waters and aqueous solutions in plastic containers for hydrogen and oxygen stable isotope analysis. *Rapid Commun. Mass. Spec.* 26(22), 2627-36.
Stefansson, A. and Arnorsson, S. (2002) Gas pressures and redox reactions in geothermal fluids in Iceland. *Chem. Geo.* 190(1-4), 251-271.
Stefansson, A., Amorsson, S. and Sveinbjornsdottir, A.E. (2005) Redox reactions and

potentials in natural waters at disequilibrium. *Chem. Geol*. 221, 289-311
Straus, J. M. and G. Schubert (1981) One-dimensional model of vapordominated geothermal systems, *J. Geophys. Res.*, 86, 9433-9438.
Stumm, W. and Morgan, J. (1996) Aquatic Chemistry: Chemical Equilibria and Rates in Natural Waters, 3rd Edition, John Wiley & Sons. New York
Symonds, R.B. and Reed, M.H. (1993) Calculation of multicomponent chemical equilibria in gas-solid–liquid systems: Calculation methods, thermochemical data, and applications to studies of high-temperature volcanic gases with examples from Mount St. Helens. *Am. J. Sci.* 293, 785–864.
Tan, C., Cino, C.D., Ding, K., and Seyfried, W. (2017) High temperature hydrothermal vent fluids in Yellowstone Lake: Observations and insights from in-situ pH and redox measurements. *J. Volcanology and Geothermal Reasearch.* 343, 263-270.
Taylor, H.P (1978) Oxygen and hydrogen isotope studies of plutonic granitic rocks. *Ear. Pla. Sci. Let.* 38 (1), 177- 210.
Truesdell, A.H., Nathenson, M., and Rye, R.O. (1977) The effect of subsurface boiling and dilution on the isotopic compositions of the Yellowstone thermal waters. *Journal of Geophysical Research*. 82, 3694–3704.
Von Damm et al. (1985) Chemistry of submarine hydrothermal solutions at 21N. East Pacific Rise. *Geochim. Cosmochim. Acta.* 49, 2221–2237.
Werner, C., and Brantley, S. (2003). CO_2 emissions from the Yellowstone volcanic system. *Geochem. Geophys. Geosyst*. 4 (7).
White, D.E., Muffler, L.J.P., and Truesdell, A.H. (1971) Vapor-dominated hydrothermal systems compared with hot-water systems. *Economic Geology.* (66) 75-97.
White, D. E., Fournier, R.O., Muffler, L. J. P., and Truesdell, A. H. (1975) Physical results of research drilling in thermal areas of Yellowstone National Park, Wyoming. *USGS Prof Pap.* 892, 1- 70.
White, D.E., Heropoulos, C., and Fournier, R.O. (1991) Gold and other minor elements associated with the hot springs and geysers of Yellowstone National Park, Wyoming, supplemented with data from Steamboat Springs, Nevada: U.S. Geological Survey Bulletin 2001, 1-19.
Wolf et al. (1989) Influence of sterilization methods on selected soil microbiological, physical, and chemical properties. J. Environ. Qual., 18, 39-44.
Wu, S. et al. (2011) A new hydraulically actuated titanium sampling valve for deep-sea hydrothermal fluid samplers. IEEE J. *Oceanic Eng.* 36, 462-469.
Xu, Y., et al. (1998) Sulfur geochemistry of hydrothermal waters in Yellowstone National Park; I. Origin of thiosulfate in hot spring waters. *Geochem. Cosmochem.* 62 (23/24), 3729-3743.
Xu, Y. et al. (2000) Sulfur geochemistry of hydrothermal waters in Yellowstone National Park, Wyoming, USA. II. Formation and decomposition of thiosulfate and polythionate in Cinder Pool. *J. Volcan. Geotherm. Rea.* 97, 407-423.
Zhang, W. and Charles, E.A. (2003) A thermodynamic approach to calculate the yttria-stabilized zirconia pH sensor potential. *J. Appl. Electrochem.* 33, p. 1025-1033.
Zohdy, A. A. R., Anderson, L. A., and Muffler, L. J. P. (1973) Resistivity, self-potential,

induced-polarization and surveys of a vapor-dominated geothermal system. *Geophysics*. 38(6), 1130-44.

APPENDIX

Alkalinity Titration

Alkalinity is the acid-neutralizing capacity of a body of water, it is the sum of all the titratable bases within the solution. When the alkalinity is entirely controlled by carbonate and bicarbonate content, the pH at the equivalence point of the titration is then determined by the concentration of carbon dioxide (CO_2), which in turn depends on the total carbonate species present. The end-point typically occurs at a pH of 4.5, which is the pKa of bicarbonate acid (H_2CO_3). It is important to consider any losses (ex. degassing effects) that may have occurred during titration. The procedure of the titration varies depending on the sample, but typically consists of incrementally adding hydrochloric acid (HCl) until you acidify the sample enough to reach a pH of 4.5.

An alkalinity titration was performed on the field in Yellowstone for each cylinder from the titanium sampler. About 5mL would be extracted from the sampler using an airtight syringe, and ejected into a plastic beaker with a stir bar on a magnetic spin plate. After the pH as taken and stabilized with a gel electrode, dilute acid of 0.015N HCl was added until the pH reached an endpoint of 4.5 The acid used to titrate the sample was prepared ahead of time back at University of Minnesota. Since the alkalinity was not known, multiple concentrations of 0.01-1N HCl were made to account for a range of alkalinities. The acid was tested on standards beforehand composed of 0.373g HCO_3, and then diluted to make a range of standards of 50-250 mg/L with alkalinity representative of the possible range of Yellowstone Lake vent fluid values.

Sulfide Conversion Procedure

Hydrogen sulfide (H_2S) concentrations were prepared by trapping the sulfide into a white crystalline zinc sulfide (ZnS) precipitate in pre-weighed evacuated amber bottle. Before extracting the ZnS precipitate, the bottles were weighed to get the mass difference to calculate the sample weight. Next, the rubber stopper sealing the amber bottle was removed, and the ZnS precipitate was separated from the fluid sample through vacuum filtration with a 0.22 μm nylon membrane filter. The filter paper with ZnS was then inserted in a glass round bottom flask with 35mL DI water, and placed in a heating mantle. The set-up used for the conversion (see Oduro et al. 2011) was purged with N_2 gas through one of the modified threaded glass septum-sealed joints for at least 20 minutes to remove molecular oxygen in the system. Concentrated acid was then injected into the round bottom flask with an air-tight syringe, volatilizing the H_2S using boiling 6N HCl. After about 10-15 minutes the H_2S begins to get trapped in 0.3M $AgNO_3$, forming Ag_2S. Anywhere from 1- 3 hours is need for the conversion to have a full yield. The Ag_2S was filtered out of the trapping solution and dried in an oven (100 °C) for gravimetric and future isotopic analyses.

Table A.1 – Location and temperature data for vent sites in Yellowstone Lake.

Latitude	Longitude	Alvin T (°C)	Sampler T (°C)	Date	Sample Name	Number
Field Ops August 2016						
44.51092	-110.35664	113	63	8/15/2016	YL16F01	SI-VF-01
44.51094	-110.35662	143	86	8/16/2016	YL16F02	SI-VF-02
44.51094	-110.35662		103	8/16/2016	YL16F03	SI-VF-03
44.5108	-110.35659		94	8/16/2016	YL16F05	SI-VF-05
44.5109	-110.35653		96-105	8/16/2016	YL16F06	SI-VF-06
44.51072	-110.35653	147	140	8/16/2016	YL16F07	SI-VF-07
44.51069	-110.35668		110-142	8/17/2016	YL16F08	SI-VF-08
44.51075	-110.35654		92	8/17/2016	YL16F09	SI-VF-09
44.51067	-110.35652		94-100	8/17/2016	YL16F10	SI-VF-10
44.51084	-110.35659		120	8/17/2016	YL16F11	SI-VF-11
44.51069	-110.35666		110-114	8/17/2016	YL16F12	SI-VF-12
44.51071	-110.35658	169	80-86	8/19/2016	YL16F13	SI-VF-13
44.51073	-110.35658	141	137-160	8/19/2016	YL16F15	SI-VF-15
44.51111	-110.35659		4	8/19/2016	BLW1	BLW 1
44.51111	-110.35659		4	8/19/2016	BLW2	BLW 2
44.51111	-110.35659		4	8/19/2016	BLW3	BLW 3
Field Ops August 2017						
44.51073	110.35654	146	150	8/10/2017	YL17F01	SI-VF-16
44.51073	110.35654		141-150	8/10/2017	YL17F02	SI-VF-17
44.51068	110.35665		142	8/13/2017	YL17F03	SI-VF-18
44.51071	110.35669		115-140	8/13/2017	YL17F08	SI-VF-23
44.51071	110.35669		143	8/13/2017	YL17F10	SI-VF-25

Table A.2 - Chemical data for metals aliquot for Yellowstone Lake vent fluid samples

Vent Sample	B (μM)	Al (μM)	V (nM)	Cu (nM)	Zn (nM)	As (nM)	Rb (nM)
YL16F01	6	5	137	4	79	177	59
YL16F02	7	10	221	17	-49	238	61
YL16F03	6	383	898	126	1753	257	66
YL16F05	6	7	271	7	78	727	36
YL16F06	6	8	253	12	494	345	48
YL16F07	6	7	264	10	102	296	69
YL16F08	9	5	250	7	14	144	59
YL16F09	5	5	259	8	41	346	46
YL16F10	6	4	756	9	52	167	61
YL16F11	6	8	249	5	132	278	55
YL16F12	8	6	119	3	53	161	53
YL16F13	8	6	2203	18	118	103	57
YL16F14	11	7	247	5	-64	156	53
YL17F01	6	0	214	31	23	23	55
YL17F02	9	6	246	30	227	245	51
YL17F03	9	0	214	14	79	233	50
YL17F08	5	4	235	10	60	140	58

Vent Sample	Zr (nM)	Mo (nM)	Ag (nM)	Cd (nM)	Sb (nM)	Cs (nM)	W (nM)	Pb (nM)
YL16F01	1	9	0	3	0	18	6	0
YL16F02	0	15	0	0	0	18	7	0
YL16F03	158	189	12	0	0	17	12	0
YL16F05	0	21	2	3	0	7	3	0
YL16F06	3	6	3	0	0	13	6	0
YL16F07	0	5	8	0	0	14	6	0
YL16F08	0	12	20	1	1	15	8	0
YL16F09	0	7	5	0	0	6	4	0
YL16F10	0	5	2	0	1	13	2	0
YL16F11	0	9	0	0	0	18	6	0
YL16F12	0	9	2	0	0	12	18	0
YL16F13	0	10	5	0	8	16	9	0
YL16F14	0	10	2	0	0	11	7	0
YL17F01	0	3	0	0	0	15	1	0
YL17F02	0	11	3	0	0	14	8	0
YL17F03	0	11	0	0	0	14	2	0
YL17F08	0	15	2	0	0	17	5	0